REPUBLIC OF TURKEY

YILDIZ TECHNICAL UNIVERSITY

GRADUATE SCHOOL OF SCIENCE AND ENGINEERING

DESIGN OF A CLIMBING ROBOT FOR CORROSION INSPECTION

ÖZGÜR ACAR

MASTER OF SCIENCE THESIS

Department of Control and Automation Engineering

Control and Automation Engineering Program

Advisor

Assist. Prof. Dr. Claudia Fernanda YAŞAR

March, 2021

REPUBLIC OF TURKEY

YILDIZ TECHNICAL UNIVERSITY

GRADUATE SCHOOL OF SCIENCE AND ENGINEERING

DESIGN OF A CLIMBING ROBOT FOR CORROSION INSPECTION

A thesis submitted by Özgür ACAR in fulfillment of the requirements for the degree of MASTER OF SCIENCE is approved by the committee on 05.03.2021 in Department of Control and Automation Engineering, Control and Automation Engineering Program.

Assist. Prof. Dr. Claudia Fernanda YAŞAR
Yıldız Technical University
Advisor

Approved By the Examining Committee

Assist. Prof. Dr. Claudia Fernanda YAŞAR, Advisor
Yıldız Technical University _____

Prof. Dr. Şeref Naci ENGİN, Member
Yıldız Technical University _____

Prof. Dr. Hasan OCAK, Member
Kocaeli University _____

I hereby declare that I have obtained the required legal permissions during data collection and exploitation procedures, that I have made the in-text citations and cited the references properly, that I haven't falsified and/or fabricated research data and results of the study and that I have abided by the principles of the scientific research and ethics during my Thesis Study under the title of Design of a Climbing Robot for Corrosion Inspection supervised by my supervisor, Assist. Prof. Dr. Claudia Fernanda YAŞAR. In the case of a discovery of false statement, I am to acknowledge any legal consequence.

Özgür ACAR

Dedicated to my family

ACKNOWLEDGEMENTS

I would like to express my gratitude for my thesis advisor, Asst. Prof. Dr. Claudia Fernanda YAŞAR, for her on-going guidance and contribution to this study. I am deeply grateful to her for her endless support and understanding at times of trouble, and for her confronting attitude towards all the potential problems.

Özgür ACAR

TABLE OF CONTENTS

LIST OF ABBREVIATION VIII

LIST OF FIGURES IX

LIST OF TABLES XI

ABSTRACT XII

ÖZET XIV

1 INTRODUCTION 1

1.1 Literature Review 1

1.2 Purpose of Thesis 2

1.3 Motivation of the Thesis 5

1.4 Objectives and Contributions of the Thesis 6

1.4.1 General Objectives 6

1.4.2 Objectives with Regards Mechanical Design 6

1.4.3 Objectives Related to the Software, Hardware, Actuation Components and Sensory System 7

1.4.4 Objectives Concerning the Programming Architecture. 7

1.4.5 Objectives Related to the Control System 7

1.4.6 Objectives Related to Applying Corrosion Inspection Tasks That Finally Allows for Proposing a Climbing Robot for Tank Inspection 8

1.4.7 Objectives Related to the Design of Motion Control with CRMS's Wheels Robust to High Perturbations 8

2 EXPERIMENTAL PLATFORM 9

2.1 Mechanical Design 9

2.1.1 Motor Torques and Magnetic Forces 10

2.1.2 Free Body Diagram 12
2.2 Sensory System 14
2.2.1 Rotary Encoder 14
2.2.2 Inertial Measurement Unit 15
2.2.3 Camera 15
2.2.4 Ultrasonic Sensor 15
2.3 Programming Architecture 16
2.3.1 Node-Red Programming 17
2.3.2 Python Programming 17
2.3.3 Arduino Programming 17
2.3.4 Cascade Trainer 18
2.3.5 Motion IP Camera Steaming Program 18
3 CONTROL SYSTEM **19**
3.1 Kinematic Model 20
3.2 Inverse Kinematic Equations 21
3.3 Sensor Fusion and Kalman Filter 22
3.4 Control Strategy of a Climbing Robot 24
3.5 Open-Loop Speed Controller 26
3.6 Closed-Loop Controller for Linear Speed and Angular Speed 27
3.7 Experimental Validation of the Control Strategy 28
4 CORROSION INSPECTION **33**
4.1 Corrosion Training and Detection with Image Camera 33
4.1.1 Cascade Training 34
4.1.2 Corrosion Detection 36
4.2 Final Test Results of Corrosion Inspection 37

5 A MOTION CONTROL STRATEGY WITH DISTURBANCE OBSERVATION FOR A CLIMBING ROBOT **38**

5.1 Introduction 39

5.2 Climbing Robot Design Characteristics 40

5.3 Control Method 41

5.3.1 DC Motor Dynamics 41

5.3.2 State-Space Model of the DC Motor and a Reduced Disturbance Observer 42

5.4 Control Method Simulation 44

5.4.1 Simulation Setup 44

5.4.2 Control Method Results 44

5.5 Conclusion 46

6 RESULTS AND DISCUSSION **48**

6.1 Conclusions with Regards the Mechanical Design 48

6.2 Conclusions Appertaining to Software, Hardware and Sensory System of the CRMS 48

6.3 Conclusion Appertaining to the Programming Architecture of the CRMS . 49

6.4 Conclusions with Regards the Design of a Control System 49

6.5 Conclusions Appertaining to Methods for Corrosion Inspection 50

6.6 Conclusions Appertaining to the Design of Motion Control for the CRMS's Wheels Robust to High Perturbations 50

REFERENCES **52**

PUBLICATIONS FROM THE THESIS **55**

LIST OF ABBREVIATION

3D	3 Dimensions
CAD	Computer Aided Drawing
CRMS	Climbing Robot Mobility Systems
DC	Direct Current
GUI	Graphical User Interface
HSV	Hue, Saturation, Value
IDE	Integrated Development Environment
IDLE	Integrated Development and Learning Environment
IMU	Inertial Measurement Unit
IOT	Internet of Things
IP	Internet Protocol
PC	Personal Computer
PD	Proportional, Derivative
PID	Proportional, Integral, Derivative
PWM	Pulse Width Modulation
TCP	Transmission Control Protocol
TOF	Time of Flight
UDP	User Datagram Protocol
USB	Universal Serial Bus

LIST OF FIGURES

Figure 1.1 a) HydroCAT b) VAL-250 c) M250 [6] 2

Figure 1.2 Examples of tank structures made of welded S355 J2 steel plates. 5

Figure 2.1 Differential wheeled robot, SolidWorks CAD drawings a) 2D isometric view, and b) 3D perspective view. 10

Figure 2.2 Differential wheeled robot, real prototype: a) Front view of a robot on the floor, and b) Climbing robot prototype on the testing vertical wall. . . . 10

Figure 2.3 Requires components of the palletized wheeled actuation system and magnetic system: a) Circle Magnet, b) Square Magnet, and c) a DC Motor, reduction and encoder. 11

Figure 2.4 Free body diagram of the of the Palletized Actuation 13

Figure 2.5 a) Rotary Encoder [11], b) IMU Sensor [12], and c) Mobius Camera [13] d) Ultrasonic Sensor [11] 14

Figure 2.6 Programming Architecture Diagram. 16

Figure 3.1 Vehicle Kinematic Model 20

Figure 3.2 1-Dimension Kalman Filter Model 22

Figure 3.3 IMU Angle Kalman Filter Results with Measured Values. 23

Figure 3.4 Head Angle of Robot with IMU and Encoder 24

Figure 3.5 Control Algorithm Block Diagram. 25

Figure 3.6 Left motor PWM commands with measured angular speed. 26

Figure 3.7 Right motor PWM commands with measured angular speed. 27

Figure 3.8 Control regulators: (a) PID scheme and (b) the use of linear speed and angular speed regulators. 28

Figure 3.9 Setting the initial point and the desired reference for tracking 28

Figure 3.10 Control performance: angular speed of the left motor. 29

Figure 3.11 Control performance: angular speed of right motor. 30

Figure 3.12 Head angle control performance. 31

Figure 3.13 Actual distance error changes. 31

Figure 3.14 Linear speed of robot, comparing desired and actual speed. 32

Figure 3.15 Rotational speed of robot, comparing desired and actual speed. 32

Figure 4.1 Example image of Corrosion.[20] 34

Figure 4.2 Example of Object Detection with Haar Cascades.[21] 35

Figure 4.3 Positive Images for Training. [22-46] 35

Figure 4.4 Negative Images for Training. [22-46] 35
Figure 4.5 Original Image for corrosion analysis. [47] 36
Figure 4.6 Gray scale image is used for cascade detection. 36
Figure 4.7 HSV coloured image, which is depicted after corrosion analysis for monitory functions. 37
Figure 4.8 Final validation of test images for corrosion inspection. [22-46] 37
Figure 5.1 Solidwork drawings of the climbing robot: (a) the system forces acting on the robot, and (b) wheels mechanism 40
Figure 5.2 Complete control method: Bezier curves, PD controller , feed-forward term, disturbance observer and its compensation, Kalman filter and the DC motor plant + disturbance. 44
Figure 5.3 Motion Control Response 46
Figure 5.4 Observer performance 46

LIST OF TABLES

Table 2.1 Magnet Specifications 11
Table 2.2 Motor Specifications 12
Table 2.3 Free Body Diagram Parameters 13
Table 2.4 List of hardware 14
Table 2.5 List of used software 18
Table 5.1 System Parameters 45

ABSTRACT

Design of a Climbing Robot for Corrosion Inspection

Özgür ACAR

Department of Control and Automation Engineering

Master of Science Thesis

Advisor: Assist. Prof. Dr. Claudia Fernanda YAŞAR

Wall-climbing robots are generally used for dangerous and expensive tasks when performed by humans due to severe conditions. The design, modelling, and control of a wall-climbing robot for tank inspection are presented in this thesis. A novel mechanical design for the system actuation based on a palletized robot with magnetic adhesion is proposed. The magnetic adhesion system is used to attach the robot to a metallic wall. The locomotion of climbing robots still represents challenges when designing control systems for each particular adhesion mechanism. The main goal is to build a light robot that includes all the required hardware, mechanism, actuators, and sensors that will allow for the use of reliable control systems and inspection tasks.

The sensor and acquisition system for robot navigation is explained in this thesis. A sensory-data strategy with a sensor fusion is used to estimate the actual position of the robot. To track the required trajectories sensor measurements and the robot kinematics are used, along with a Kalman filter, which, in turn, would enhance the motion control strategy, making the system robust to the possible disturbances and noise. A camera-based inspection system is part of the sensory system but is used for inspection purposes.

The robot system was designed with the capability of climbing metallic vertical sheets. Experiments confirmed a successful performance of system mechanics, sensory fusion strategy, and the control performance for robot locomotion and adhesion. This climbing robot has demonstrated the capability to follow an accurate reference on a vertical wall. The robotic application is endowed with a camera system that can detect, process, classify corrosion figures, and present classification results on a monitory diagnostic system.

Finally, to fulfil the high robustness requirements, a control method is based on the design of a PD controller and an observer, in which the overall disturbance, Coulomb friction, and sudden changes of the inertia, are estimated and then compensated. A robust motion control strategy for the climbing robot mobility that uses DC motors is explained. This method is part of a preliminary study to design advanced motion controllers for a climbing strategy. The controller is still under development, but some designs from the availed literature and initial simulations have been performed with successful results. Simulations of the control strategy were carried out using Matlab/Simulink. Further work aims at validating advanced control methods for climbing robots under high disturbances coming from magnetic, Coulomb, and gravity forces.

Keywords: Climbing robot, corrosion inspection, position estimation, motion control, non-destructive testing

ÖZET

Otonom Tırmanan Korozyon Denetleme Robotu

Özgür ACAR

Kontrol ve Otomasyon Mühendisliği Anabilim Dalı

Yüksek Lisans Tezi

Danışman: Dr. Öğr. Üyesi Claudia Fernanda YAŞAR

Tırmanma robotları, insanlar tarafından zorlu koşullarda yapılan, genellikle tehlikeli ve maliyetli olan işler için kullanılır. Bu tezde, tank incelemesi için bir tırmanma robotunun tasarımı, modellemesi ve kontrolü sunulmuştur. Manyetik kuvvete sahip paletli bir robota dayanan sistem için yeni bir mekanik tasarım önerilmektedir. Robotu metal bir duvara sabitlemek için manyetik kuvvet kullanılır. Kontrol sistemleri tasarlarken her bir tutunma mekanizması için tırmanma robotlarının hareketi, hala büyük zorlukları temsil etmektedir. Ana hedef, güvenilir kontrol sistemlerinin ve denetim görevlerinin kullanımına izin verecek, tüm gerekli donanımı, mekanizmaları, aktüatörleri ve sensörleri içeren, olabildiğince hafif bir robot tasarlamaktır.

Robot navigasyonu ve tank kontrolü için sensor sistemi açıklanmıştır. Mutlak robot konumunu tahmin etmek için bir sensör füzyon sistemi stratejisi olarak sunulur. İstenen yörüngeleri doğru bir şekilde izlemek için, sensör ölçümleri ve robot kinematiği, gerçek robot konumunu tahmin etmek için bir Kalman filtresi ile birlikte kullanılır. Bu sensor füzyon sistemi, hareket kontrol stratejisini geliştirmek için kullanılmaya uygundur ve özellikle sistem olası rahatsızlıklara ve gürültüye

karşı sağlam olmalıdır. Kamera tabanlı bir tank korozyon denetim sistemi, istemci/sunucu mimarisine dayanmaktadır.

Robot konfigürasyonu, kamera inceleme görevleri için çelik duvarlara tırmanma özelliğiyle geliştirilmiştir. Çoklu deneyler, tüm sistem mekaniğini, sensör füzyon stratejisinin kullanımını ve robot hareketi için kontrol sistemi performansını doğrular. Bu robotik sistem, dikey bir duvarda doğru bir yörünge izleme ve görsel bir inceleme gerçekleştirme yeteneğini göstermiştir. Robotik uygulama, korozyon resimlerini algılayabilen, işleyebilen, sınıflandırabilen ve bir izleme tanı sistemi üzerinde sınıflandırma sonuçlarını sunabilen bir kamera sistemine sahiptir.

Son olarak, kararlılık ve yüksek sağlamlık gereksinimlerini karşılamak için, bir kontrol yöntemi, genel bozulma, Coulomb sürtünmesi ve ataletin ani değişikliklerinin tahmin edildiği ve ardından telafi edildiği bir PD kontrolörü ve bir gözlemcinin tasarımına dayanır. DC motorları kullanan tırmanma robotu hareketliliği için sağlam bir hareket kontrol stratejisi açıklanmıştır. Bu, tırmanma stratejisi için gelişmiş hareket kontrolörleri tasarlamaya yönelik bir ön çalışmadır. Yöntem hala geliştirme aşamasındadır, ancak mevcut literatürden bazı kontrol tasarımları ve ilk simülasyonlar başarılı sonuçlarla gerçekleştirilmiştir. İzleme performansı için tam kontrol yönteminin simülasyonları Matlab/Simulink kullanılarak gerçekleştirildi. Daha fazla çalışma, manyetik, Coulomb ve yerçekimi kuvvetlerinden gelen yüksek bozulmalar altında tırmanma robotları için gelişmiş kontrol yöntemlerini doğrulamayı amaçlamaktadır.

Anahtar Kelimeler: Tırmanan robot, korozyon denetleme, pozisyon kestirimi, hareket kontrolü, tahribatsız muayene

1

INTRODUCTION

This chapter presents an outline of Climbing Robot Systems (CRMS), providing a review of the main areas. The information in this chapter focuses on climbing robots technologies used to enhance functional mobility. This information can be used to motivate the proposed work and to define the objectives of this thesis.

General topics about climbing robots are discussed in this chapter, such as the motivation of this research, along with general and specific objectives. This chapter includes a brief state of the art on climbing robots. Some considerations and assumptions to describe robotic mechanisms for climbing, a redundant sensory system, and the control strategy are cited.

The chapter is outlined as follows: Section 1.1 reviews relevant literature on CRMS. Section 1.2 presents aspects of the design, control and some factors that prevent their design progress. Section 1.3 explains the motivation. Section 1.4 provides the main objectives and contributions of this work.

1.1 Literature Review

Wall-climbing robots are used for risky tasks when an inspection has to be performed by people due to severe working circumstances. The required jobs are multiple that includes storage tanks maintenance, the examination of large concrete, and evaluation in narrow places. An essential part of the wall-climbing robot's design is the adhesion mechanism [1].

Climbing robots are mobile systems that can work on high surfaces performing different jobs, such as cleaning, construction work, painting, and inspecting storage in which robotic systems are required since the job is dangerous for human operators. A large number of robots design for climbing vertical surfaces have been developed. These robots can be classified into two roles locomotion and adhesion [2]. Climbing robots can attach to a surface using suction and magnetic

force, using micro-spines for interlocking, and Van der Waals forces. Mechanisms with magnetic forces are available when the climbing surface is made of ferromagnetic materials [3]. The motion of climbing robots still represents challenges when planning control systems for each particular adhesion system.

The main goal must be designing a light system that includes all the hardware, mechanisms, actuators, and an inspection system that will allow for using reliable control systems. Potential risks must be considered to ensure correct functionality. This analysis incorporates safety considerations and the prospect that components within the robot may break, which also accounts for the risk of plastically deforming components around the climbing area, and the case of the robot falling or slipping [4]. The last two decades show dramatic progress in the application of climbing systems [5] and an increasing variety of commercial robots [6]. Figure 1.1 shows some examples of climbing robots.

Figure 1.1 a) HydroCAT b) VAL-250 c) M250 [6]

Many procedures are performed for high ship hulls with enormous surface areas. Some of the required tasks are tedious and potentially dangerous, for instance, removal of rust, stripping of coatings and corrosion inspection, cleaning of weld seams [2]. Staff on aerial working platforms [3] do most of these operations manually. Some climbing robots that are capable of climbing vertical surfaces have been developed all over the world [7] [8].

1.2 Purpose of Thesis

The adhesion mechanism provides the holding capability of the device on the vertical wall or ceiling [6]. A worthy example is a magnapod design that are wall-climbing legged robots, designed for electro-magnetic inspection, very useful in confined inspection tasks and capable of carrying up to 10-kilogram sensor

payload [7]. The magneto is a versatile multi-limbed quadruped inspection robot with a compact magnetic foot design of footprint, which allows for walking on narrow beams of thickness. The inherent high dimensional system enables the body to be positioned in a wide range of orientations and with a switch function from locomotion to manipulation mode mid-climb. This capability enables access to confined space openings and occluded pockets and navigation through complex 3D structures, a not demonstrated characteristic on legged climbing robots, previously. On the other hand, some other mechanisms allow climbing robots to attach themselves on the wall by using suction force, magnetic forces, electrostatic and elastomer adhesion.

Permanent magnetic adhesion and tracked locomotion mechanisms are often employed in wall climbing robot systems [8]. Multiple wall climbing applications have been proposed in the literature, among them, the low-cost robot designed by Dartmouth College students to climb a near-vertical indoor climbing wall using force feedback to maintain pressure on handholds [9]. Using a variation of a probabilistic roadmap algorithm, the climbing route up the wall is planned and then executed. Another example is robot prototypes based on electrostatic and elastomer adhesion that can climb a slope of 80° on smooth surfaces. This work demonstrates that the elastomer material properties for the hybrid adhesive are suitable for a stable climb on vertical surfaces [10].

The design of DC servo-motor regulators has been one of the bases of mechatronics and multiple applications in the industry [11]. A well-designed motion controller for climbing robots requires proper selection of several devices for sensing and actuation, as well as efficient control algorithms. Robust, precise and fast motion is the main target for a climbing robot movement. In order to compensate the plant nonlinear phenomena the estimation and compensation of the overall disturbances become essential for the control system performance [12][13]. Innovative methods for disturbance compensation based on observers are well described [12], [14], among others. Nonlinear position-tracking controllers with a disturbance observer have been proposed to track the desired position in the presence of the disturbance that affects electrohydraulic actuators.

The design of robust servo-motor control with switched observers [15], illustrates enhanced performance because it compensates for un-modelled classical perturbation inputs that affect the observed plant since it exhibits dynamic output reconstruction error injections.

In this thesis, a climbing robotic application is designed for the inspection of tanks that are made out of thin ferromagnetic sheets. Some mechanical prototypes of the proposed CRMs are therefore explained; it includes a description of the mechanism, servo-motors and transmission system, the tracked locomotion system, and permanent magnetic adhesion wheels. Since adhesive force and Coulomb friction are all changing in nonlinear patterns, the interaction process must experience strong nonlinearities [6]. Nonlinear phenomena of the Coulomb friction and the effects of gravity have a strong influence on climbing robots making it very difficult to control the robot's wheels accurately [12].

The CRMs system was designed and built, this study considers the dynamics of wheels, kinematics of the overall robot, the sensory system for system positioning, and a Kalman filter that estimates system actual posıtion making use of a sensor fusion strategy. Multiple experiments for parameter identification were performed to finally design controllers for the system locomotion. Experimental characterization of the CRMs allows for designing some basic algorithms that provide the system with speed and position control, and the localization of the system in his working environment.

The final part of this work shows the design and simulation of motion controllers for the magnetics wheels of a robot. This includes a compensation term for the uncertain nonlinear static friction due to the changes of the control forces of linear and non-linear nature [13]. The system is modelled and based on an augmented state model. The controller method is designed to handle the unknown overall load disturbance and uncertain nonlinearity coming from friction, gravity and magnetic forces as a whole. The effectiveness of the proposed control for the suppression of largely unknown disturbances has been studied by performing simulations using Matlab/Simulink. The proposed approach guides the prospect of robust motion control algorithms for climbing robots in our future work.

1.3 Motivation of the Thesis

Climbing robots use multiple sensors for efficient navigation. These sensors are placed in specific locations on the robot for data collection [16]. They provide measurement and feedback from the operating state of the system and its working environment.

The climbing robot can be placed on vertical metallic structures for inspection tasks. However, the most common use is in tanks, steel structures or metallic high-rise industrial buildings. Structures must be checked according to national and international standards regarding occupational safety and continuous provision of infrastructure services.

The maintenance of these facilities consists of non-destructive tests, such as visual inspection, wall thickness measurement, welding controls, etc. However, because the structures are large and high, the way to address structural inspection points or areas is crucial. Safety risks and economic aspects must be evaluated. The idea of using robots for inspection employing cameras, thickness gauges, ultrasound sensors incorporated in a robot has many advantages. Among the measurements to determine the remaining structure life, the wall thickness is mandatory, because it is an indirect indicator of corrosion. Visual inspection is important because of possible deformation on the weld and to analyse the structure condition at the base.

A real scenery can be described as a climbing robot for tank inspection. This tank may keep gas, oil, and chemical or water for infrastructure services. In Figure 1.2, two examples of real tanks are illustrated, in which the Tanks' walls are made of welded S355 J2 steel plate, and the thickness, (under standard conditions) is 10-15 mm. The walls do not have any coating but are painted for corrosion protection.

Figure 1.2 Examples of tank structures made of welded S355 J2 steel plates.

1.4 Objectives and Contributions of the Thesis

1.4.1 General Objectives

In this thesis, a CRMS is developed, the work includes a control strategy to drive the robot on a metallic vertical wall. Multiple mechanical, electronic, computational and control studies must be performed to design a robot:

- Design of the system mechanics, parts, selection of motors and the actuation system.
- Design a mobility strategy based on magnetic adhesion.
- Drive the system under the effects of the gravity, high magnetic force coming from the adhesion wheels, and the Coulomb friction forces of linear and nonlinear nature.
- Design a sensory system to measure parameters about the system environment and locomotion.
- Generate the trajectories for the robot positioning and design controllers for the system mobility and inspection.
- Apply a visual inspection task to validate our designs.
- Design a control strategy that allows for driving vertical metallic surfaces.

1.4.2 Objectives with Regards Mechanical Design

- To design CAD models in SolidWorks that will permit the fabrication of its parts.
- To design actuation mechanisms for the positioning and climbing, all the constitutive parts for manufacture and assembly.
- To select the DC motor as part of the actuation system and evaluate performance considering the system is subjected to inertia changes, friction and gravity effects that causes saturation in the actuators.
- To design climbing mechanisms to adapt the system for climbing on a vertical sheet. It includes the required components for the magnetic adhesion.
- To ensure a stable posture of the robot and ensure safety which involves designing and redesigning some parts.
- To validate the performance of mechanical designs, and the study the advantages and disadvantages.

1.4.3 Objectives Related to the Software, Hardware, Actuation Components and Sensory System

- Implement the necessary hardware, software and communication algorithms.
- The development of a redundant sensory system for robotic locomotion, to measure system positioning, and to be used for control feedback. The fusion sensor strategy based on motor encoders, ultrasound sensors, capacitive sensors, time of flight sensors (TOF) and a camera system.
- Experimental verification of the sensory system. Experiments will be carried out using sensors onboard for locomotion and calibration system.
- To validate the sensory fusion, the use of encoders, IMU sensors, as measurements needed to obtain head-angle and overall system positioning, to be used for the control system.
- To design and program a Kalman filter to be used along with the sensory system for generating the necessary trajectories. The validation of the Kalman filter and the evaluation of performance.

1.4.4 Objectives Concerning the Programming Architecture.

- To design an efficient and flexible programming architecture.
- To implement a Node-Red architecture that allows for reconfiguration of control and acquisition algorithms. This must include communication algorithms for the hardware, the communication between applications, and getting the required data from the sensor system.
- To develop Node-Red, a web-based red with easy IOT integration abilities that can work with other programs integrated into the structure. It must allow for connecting an Android tablet to get multiple measurements coming from the sensory system, and manual manoeuvre by using a joystick.
- To develop a state machine and flow logic for the control system and that allows for easy configuration based on the information from the sensory system.

1.4.5 Objectives Related to the Control System

- To design and implement control algorithms based on differential driving for the autonomous CRMS.

- To propose a way-point planning method that is suitable for climbing vertical surfaces. It has been denominated way-point tracking because the system generates a series of coordinated steps to reach a final desired (X,Y) coordinate. There are multiple points that are used as a target for the mobility system, points that are continually measured by the sensory system and give feedback to the controller and monitory system.
- To perform experimental characterization of the robotic actuation system to be able to use it for control purposes.
- To generate filtered references using the sensory fusion, system kinematics, and a Kalman filter to plan the required way-point.
- To design a complete control strategy based on PID closed-loop control for linear speed and angular speed. It will give to the robot the required control positioning to correct its head angle when performing a way-point.
- To test the performance of the complete control considering the way-point tracking error, sensors performance and control effort measurement.

1.4.6 Objectives Related to Applying Corrosion Inspection Tasks That Finally Allows for Proposing a Climbing Robot for Tank Inspection

- To develop a camera-based method that obtains pictures of the climbing surface, use image-processing algorithms and feature classification to identify corrosion areas while the robot is climbing.

1.4.7 Objectives Related to the Design of Motion Control with CRMS's Wheels Robust to High Perturbations

- To study and design an efficient control system when the dynamics are not known, and disturbances are changing, since friction in the actuator varies with time, the actuators may saturate, and changes with regards the robot' head-angle affect the system.
- To propose and simulate a motion control method for the robot's wheels robust to high perturbation values has to be simulated to fulfil the stability and high robustness requirements when subjected to magnetic, Coulomb friction, and gravitational forces.

2

EXPERIMENTAL PLATFORM

This chapter explains the climbing robot prototype. It describes the experimental platform's mechanical design and programming architecture. The description includes mechanisms for the climbing, the required magnetic adhesion method, and sensory system. The proposed mechanics is based on a model that aims at avoiding the sliding problem. A brief description of the programming architecture used to program all our algorithms is presented. The programming architecture uses a Node-Red which provides a flow structure with IOT integration abilities and works with many other programs. It allows for linking and programming control, communication and inspection algorithms to the main program.

Section 2.1 defines the system mechanics and a free body diagram of the climbing robot to calculate the required magnetic forces, while in Section 2.2, the sensory system is described. Finally, Section 2.3 describes programming architecture.

2.1 Mechanical Design

The Climbing Robot experimental platform was fabricated at the Control and Automation Engineering Department, Electrical and Electronics Engineering Faculty, Yildiz Technical University. The SolidWorks CAD drawings and photos of the real prototype are shown in Figure 2.1 and Figure 2.2. This differential wheeled robot is driven to provide the required climbing posture using positioning controllers. The differential mobility system uses palletized wheels (shown in Figure 2.1 and Figure 2.2) with neodymium magnets and magnetic rubber frames.

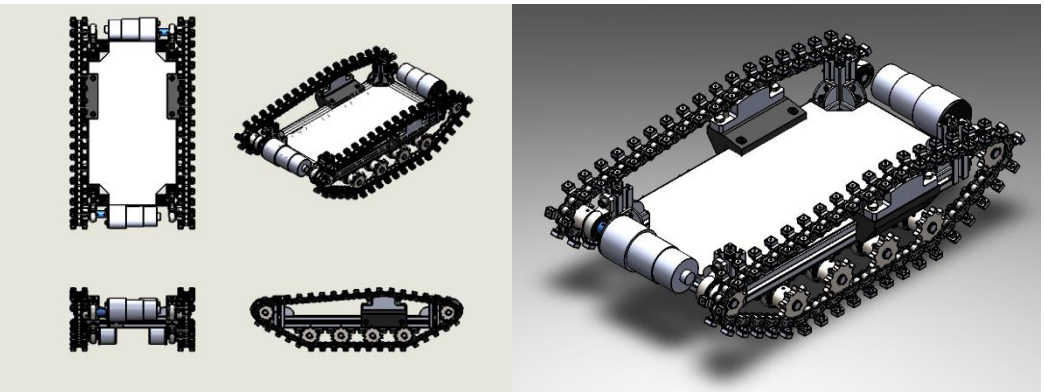

(a) (b)

Figure 2.1 Differential wheeled robot, SolidWorks CAD drawings a) 2D isometric view, and b) 3D perspective view.

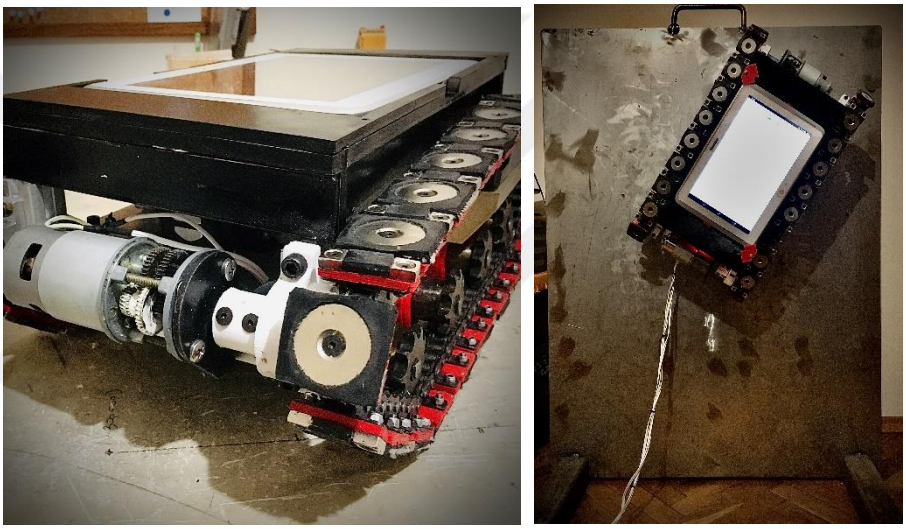

(a) (b)

Figure 2.2 Differential wheeled robot, real prototype: a) Front view of a robot on the floor, and b) Climbing robot prototype on the testing vertical wall.

2.1.1 Motor Torques and Magnetic Forces

The palletized actuation system uses two types of neodymium magnets and powerful DC motors with high torques and provides reductions and encoder sensors. Specifications of the required magnets are written in Table 2.1, Figure 2.3(a) and Figure 2.3(b) are pictures of the required magnets, and Figure 2.3(c) shows a picture of a DC motor.

Table 2.1 Magnet Specifications

Circle Magnet Parameters	**Value**
Grade	$N35$
Outer Diameter	30 mm
Hole Diameter	10 mm
Thickness	5 mm
Distance from metal surface	0.5 mm
Pull Force at Magnet to a Steel Plate	65 N[9]
Square Magnet Parameters	
Grade	$N35$
Length and Width	30 mm
Hole Diameter	10 mm
Thickness	5 mm
Distance from metal surface	0.5 mm
Pull Force at Magnet to a Steel Plate	8 N [9]

(a) (b) (c)

Figure 2.3 Requires components of the palletized wheeled actuation system and magnetic system: a) Circle Magnet, b) Square Magnet, and c) a DC Motor, reduction and encoder.

The complete system makes use of 38 circular magnets and 80 square magnets. However, while climbing, there are 10 circle magnets and 20 pieces of square magnets in permanent contact with the surface. Therefore the overall magnetic forces is $F_{Magnet,\ Total}$=810 N. The palletized actuation system uses two motors to generate the tracking forces. Specifications of motors are shown in Table 2.2.

Table 2.2 Motor Specifications

Left Motor Parameters	**Value**
Working Voltage	$0 - 24\ V$
Max Speed	$27\ rpm$
Max. Torque	$8\ Nm$
Shaft Diameter	$8\ mm$
Right Motor Parameters	
Working Voltage	$0 - 12\ V$
Max Speed	$6\ rpm$
Max. Torque	$8\ Nm$
Shaft Diameter	$8 \quad mm$

2.1.2 Free Body Diagram

In Figure 2.4, a free body diagram illustrates the required forces, as follows:

- The minimum magnetic force is the force required to keep the climbing robot on the metal sheet.
- The minimum torque is the rotational force that allows for moving the robot on the metal sheet.

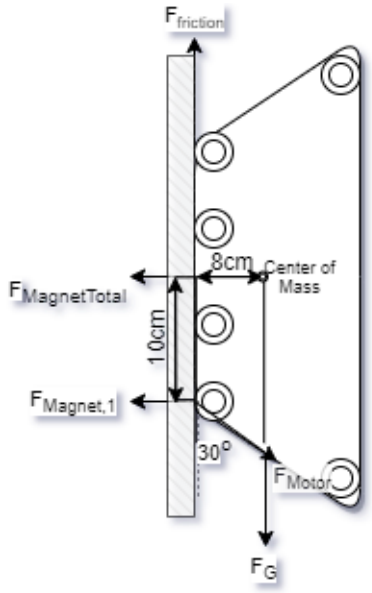

Figure 2.4 Free body diagram of the of the Palletized Actuation

Table 2.3 Free Body Diagram Parameters

Parameters	**Value**
Weight of Climbing Robot	10.5kg
Weight of 100m Power Cable(2x2.5TTR)	13.3 kg [10]
Total Weight (F_G)	23.8 kg
Biggest Magnetic Force for ($F_{Magnet,1}$)	65 N
Total Magnetic Force ($F_{Magnet,Total}$)	810 N
Radius that is connected shaft (r)	22.5 mm
Coefficient of friction between rubber and steel (μ)	0.64

The Minimum motor torque calculation is obtained as follows:

$$F_{Magnet,1} * 10 \; + \; F_G \cdot 8 = \; F_{Motor} \cdot Sin(30) \cdot 10 \qquad (2.1)$$

Which means that each DC motor should provide at least a minimum torque of 5.3 Nm. The required minimum magnetic force to avoid of sliding is $F_{friction}$:

$$F_{Friction} = N \cdot \mu = F_G \tag{2.2}$$

Therefore, the needed minimum magnetic force is 364 N.

2.2 Sensory System

The sensory system must provide support for robot system positioning, the required wheel position for way-point tracking, in addition to a camera system for corrosion inspection. The sensory system for positioning uses rotary encoders, IMU sensors. Figure 2.5(a) and Figure 2.5(b) shows pictures of the selected sensors. On the other hand, the corrosion inspection uses a Mobius Camera as shown in Figure 2.5(c). For obstacle avoidance and ground information, the system uses ultrasonic sensors shown in Figure 2.5(d). In table 2.4, a list of hardware is detailed.

(a) (b) (c) (d)

Figure 2.5 a) Rotary Encoder [11], b) IMU Sensor [12], and c) Mobius Camera [13] d) Ultrasonic Sensor [11]

2.2.1 Rotary Encoder

Incremental encoders are mechanically connected to the pallets and in charge of measuring each chain movement (one encoder per pallet). It measures the rotational positions, and in turn, the pallet rotational speed is obtained. Pallet positions and speeds are measured to obtain the actual position of the climbing robot.

2.2.2 Inertial Measurement Unit

IMU sensor LSM330DLC includes 3-axis gyroscope and iNemoEngine orientation. This IMU is placed on the top of the frame of the climbing robot, to provide measurements of the robot orientation.

2.2.3 Camera

A Mobius Action Wide Angle Camera is used for the inspection system that provides pictures of the metallic surface and corrosion samples to be processed and worked along with machine learning algorithms.

2.2.4 Ultrasonic Sensor

Ultrasonic sensors are mechanically are located to every corner of the frame to show the front, the side and the down. There is 1 ultrasonic sensor for each side, and there are 6 ultrasonic sensors. The climbing robot has obstacle avoidance ability with the front and the side sensors and has an understanding of ground with the down sensors. The climbing robot can work autonomously by using these ultrasonic sensors.

Table 2.4 List of hardware

Hardware Name	**Purpose**
Raspberry Pi 3b+ (1 piece)	Main board
Arduino Nano (2 pieces)	Produces PWM signals for motor drivers and reads rotary encoder
VNH2SP30 (2 pieces)	Motor driver, and it works with PWM signals
Arduino Nano (1 piece)	Read ultrasonic sensors

2.3 Programming Architecture

In this thesis, the main program of the designed architecture is shown in Figure 2.6. A Node-Red is web-based and has easy IOT integration abilities, and works with other programs integrated into the structure. This system makes use of Arduino for motor driving and a Node-Red integration method with RS-232 serial communication getting inputs from the sensory system. Also, Python with OpenCV libraries is integrated for image processing. The system uses Linux execute commands at Node-Red to work Python Script of image processing.

An android tablet is provided to get multiple measurements coming from the sensory system. The measured values feed the Node-Red by UDP Socket. Furthermore, there are manual operating options to drive the robotic system. It is possible because of the client Node-Red application that works on a user Windows PC. A joystick is connected to a computer and allows for manual manoeuvre. The joystick commands are integrated using Node-red via TCP-Socket. Finally, the system has a web-based user-interface and users can be connected to the robot via mobile phone or a pc. The climbing robot and the user are connected to the same wireless network. In Figure 2.6, the programming architecture's diagram is illustrated. In Table 2.5, a list of used software is detailed.

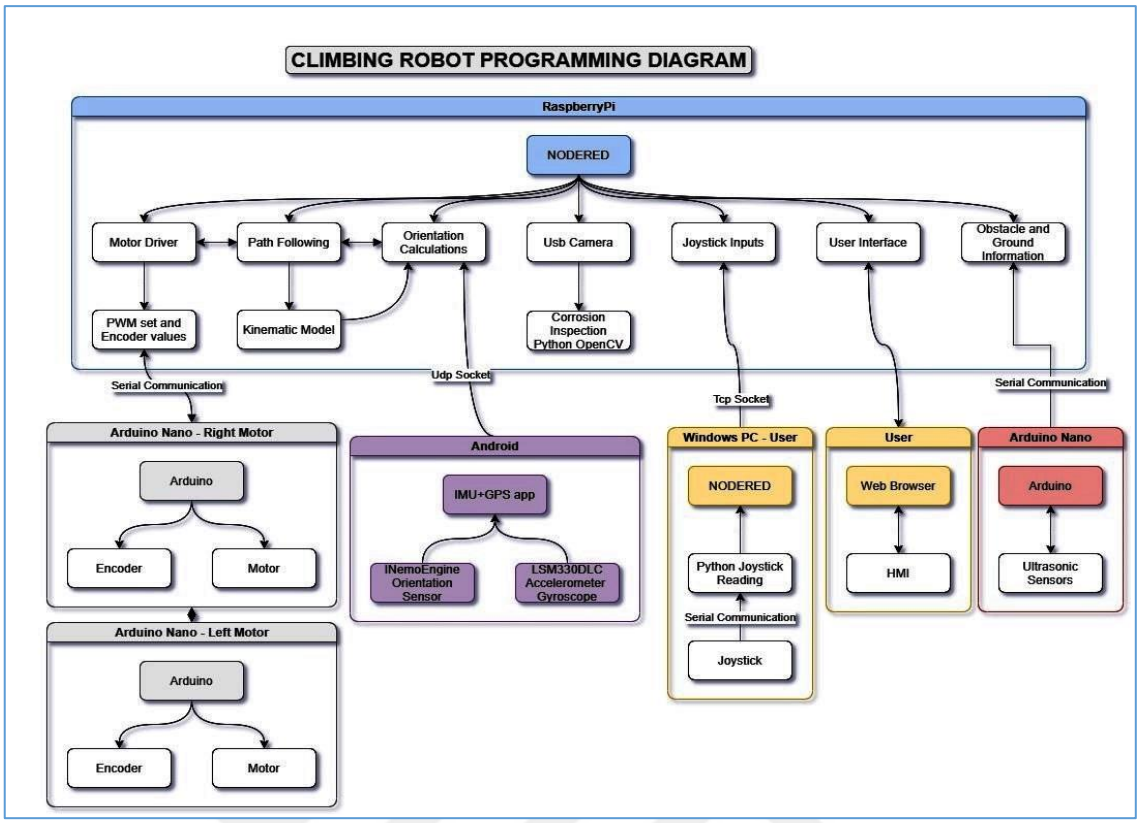

Figure 2.6 Programming Architecture Diagram.

2.3.1 Node-Red Programming

This work in this thesis use Node-RED which is a programming tool that links all the required hardware. This tool offers a browser-based editor to wire flows and nodes in a kind of palette and allows for deploying runtime. JavaScript functions were used with a flexible library that allows for saving functions, templates, and flows [14].

2.3.2 Python Programming

Python was the programming language because it offers simple and efficient high-level data structures for object-oriented programming [15]. Python and OpenCV tools were for training and testing corrosion inspection images.

2.3.3 Arduino Programming

Arduino programming and microcontrollers were used because of the advantages of open-source hardware and software. In this project, we took the advantage of available microcontroller kits in the market, and the large number of programs that the Arduino community offers [16].

2.3.4 Cascade Trainer

Cascade Trainer GUI was used to train, test, and improve cascade classifiers. The use of a graphical interface allows for setting the parameters and using OpenCV tools for training and testing different classifiers [17].

2.3.5 Motion IP Camera Steaming Program

Motion IP was used to monitors video signals from the cameras, converting a Mobius USB camera to convert into an IP camera [18].

Table 2.5. List of used software

Software Name	**Purpose**
Node-Red	Main program
Arduino IDE	Input-Output signal processing
Motion	IP camera streaming
Cascade-Trainer-GUI	Cascade trainer for corrosion detection
Python IDLE	Image processing and joystick integration

3

CONTROL SYSTEM

A detailed design of mechanisms, magnetic system to attach the robot's body to the metallic wall, and the sensory system has been explained in the previous chapter, along with the necessary programming architecture used for this robotic application. A control system for motion positioning is proposed in this chapter, which integrates sensor measurement and acquisition for navigation and control. This system is powered by a sensor fusion strategy that includes IMU sensor and encoder measurements that work with a Kalman filter, making the design suitable to be used for robot motion positioning, making the system robust to the disturbances and noise. These measurements are used to estimate the absolute position of the robot.

The sensor fusion and the robot kinematics are used for accurate way-point tracking. It is an advantage when designing a control method for a climbing strategy. Numerous experiments were carried out, which guided us to the prospect of controlling the robotic system under challenging manoeuvres when climbing a metallic surface. Experiments confirm the successful performance of redundant sensors, and in turn, the use of a Kalman filter to improve control responses and its usage in the overall control performance.

This chapter is outlined as follows: Section 3.1 describes the kinematic model of the climbing robot and is used to calculate localisation parameters. Section 3.2 describes the inverse kinematic to understand how to convert the desired speed references into the required control signals. In Section 3.3, the sensor fusion and Kalman Filter is explained. Section 3.4 explains a control strategy based on a closed-loop position and angle controller. Section 3.5 provides a description of an open-loop speed controller, and the use of lookup tables for the position control strategy. The closed-loop controllers for linear speed and angular speed are commented in Section 3.6. Finally, in Section 3.7, a description of the main experimental results of the control strategy.

3.1 Kinematic Model

Kinematic model and the sensor fusion are used to estimate the robotic body's head angle (direction angle of the robot). This angle is measured using IMU sensors and feed the control algorithm in order to provide an accurate path following. The kinematic equations and IMU sensor values are also used for both the control system and the Kalman filter, providing the required information to track a way-point.

This thesis describes a differential-drive climbing robot; therefore, the kinematic model of differential drive robots is used, as shown in Figure 3.1. Here, the radius of rotation is R, the rate of rotation is stated as ω, the instantaneous centre of curvature is written as ICC, wheel velocities are V_l, V_r, the climbing robot length is denoted by L, and V stands for the forward velocity.

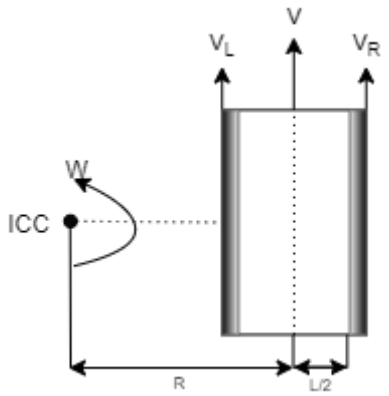

Figure 3.1 Vehicle Kinematic Model

The following are the main kinematic equations:

$$\omega = \frac{V_r - V_l}{L} \tag{3.1}$$

$$V = \frac{V_r + V_l}{2} \tag{3.2}$$

Wheel velocities V_l, V_r, can be calculated based on wheel radius r and rotational speeds ω_l, ω_r:

$$V_l = \omega_l \cdot r \tag{3.3}$$

$$V_r = \omega_r \cdot r \tag{3.4}$$

Using of (3.3) and (3.4) on (3.1) and (3.2) gives:

$$\omega = \frac{r \cdot (\omega_r - \omega_l)}{L} \tag{3.5}$$

$$V = \frac{r \cdot (\omega_r + \omega_l)}{2} \tag{3.6}$$

These kinematic equations are used to get angular and linear speeds of the climbing robot. These values are used to estimate the location of the climbing robot in real-world coordinates. The desired location is given using (x, y) parameters, and the heading (θ) of the climbing robot, considering an X-Y coordinate system that is described using the following equations:

$$\theta' = \omega \cdot T_s \tag{3.7}$$

$$X' = V \cdot Cos(\theta') \cdot T_s \tag{3.8}$$

$$Y' = V \cdot Sin(\theta') \cdot T_s \tag{3.9}$$

Using these position and angle parameters, the varying position of the robot can be calculated:

$$X = X + X' \tag{3.10}$$

$$Y = Y + Y' \tag{3.11}$$

$$\theta = \theta + \theta' \tag{3.12}$$

3.2 Inverse Kinematic Equations

Rearranging (3.5) and (3.6):

$$\omega_r - \omega_l = \omega \cdot \frac{L}{r} \tag{3.13}$$

$$\omega_r + \omega_l = V \cdot \frac{2}{r} \tag{3.14}$$

$$\omega_l = \frac{V - \omega \cdot \frac{L}{2}}{r} \tag{3.15}$$

$$\omega_r = \frac{V + \omega \cdot \frac{L}{2}}{r} \tag{3.16}$$

(3.15) and (3.16) give required motor speeds for specific left and right angular speed of robot.

3.3 Sensor Fusion and Kalman Filter

The accurate position estimation during the path execution phase is very important to minimize errors in the control system. In order to deal with localization issues, robots use additional or redundant sensors; therefore, in this application, the system is enhanced with encoders and IMU sensors. A sensor fusion must provide better results than a single sensor [19].

In order to implement the sensor fusion, an INemoEngine Orientation sensor is used to get the head angle of robot, and an LSM330DLC gravity sensor (Accelerometer, Magnetometer, 3 Axis) to measure and distinguish when the climbing robot is working on the vertical or horizontal state. When the z-axis of the gravity sensor is less than 5m/s2, the robot works in a horizontal way. If z-axis of gravity sensor is greater than 5m/s2, the robot works in a vertical way. This information changes the used INemoEngine orientation sensors values. When the robot works on a horizontal surface, the pitch angle is used for the head angle. However, if the robot works on a vertical, the yaw angle is used for the head angle.

The Kalman filter works predicting states and updating of states, as depicted in Figure 3.2. There are two parameters to consider in a Kalman filter, Q is the process noise and R is an error in the measurement. In this case, the values of these parameters are $Q = 0.001, R = 2$, which are the best suitable values obtained by means of experiments.

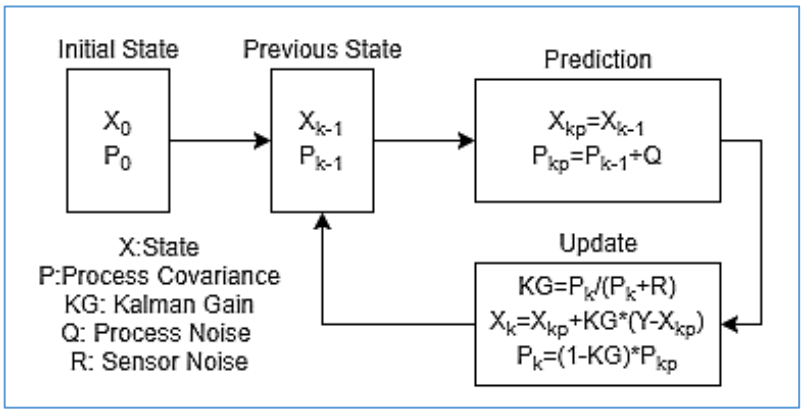

Figure 3.2 1-Dimension Kalman Filter Model

In Figure 3.3, the measured IMU angle and filtered values obtained when applying the Kalman filter are shown. This experiment validates the use of the Kalman

filter, the filter gives a fast and accurate estimation of the measured values, and the absolute error is about two (2) degrees when the steady state is reached.

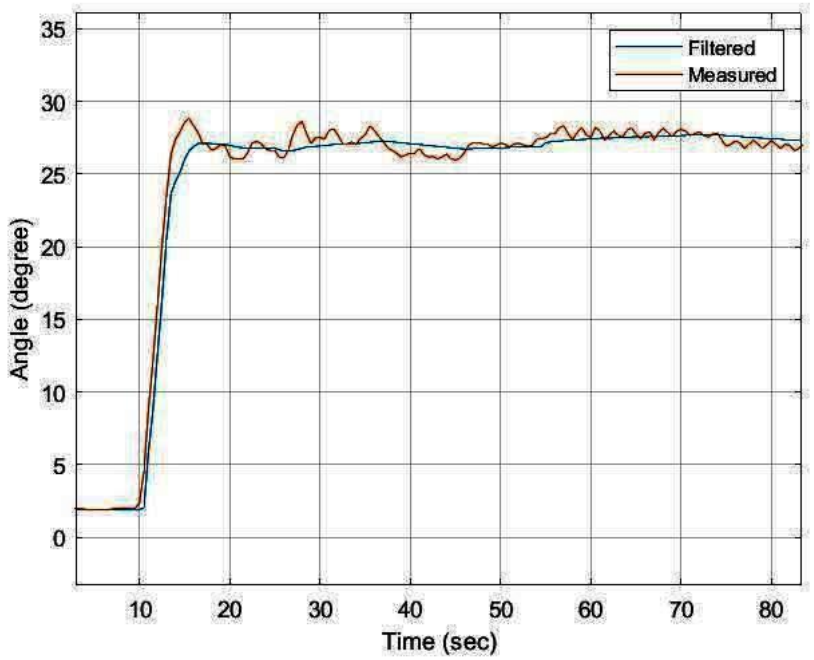

Figure 3.3. IMU Angle Kalman Filter Results with Measured Values.

With sensor fusion, the filtered head angle is calculated using both encoders and IMU sensor measurements. Figure 3.4 shows a comparison of both results, in which each filtered head angle is compared. The head angle using IMU sensors and encoder angles are depicted in this figure. The results are very similar, but the head angle estimation by means of IMU sensor presented stable values to be used to feed it back to the control system. The picture presents an offset that can be easily eliminated by software.

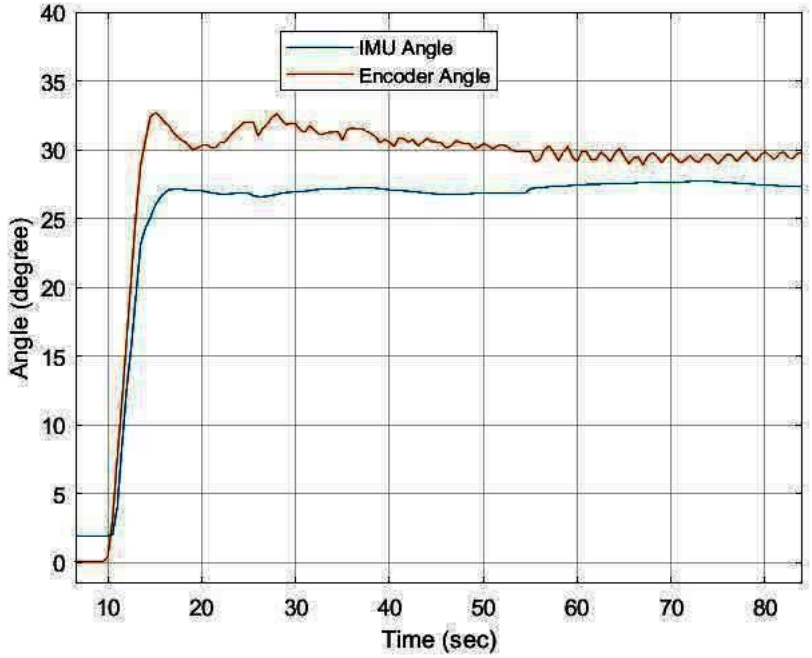

Figure 3.4 Head Angle of Robot with IMU and Encoder

3.4 Control Strategy of a Climbing Robot

In this section a control strategy for a differential driving robot is depicted. Multiple experiments are performed to validate the system performance. Figure 3.5 is a block diagram of the full strategy.

The control strategy for path following starts with desired X and Y positions as coordinates. The X ,Y target position are constantly compared to actual positions, then position and angle controllers try to minimize this error. Every position error is calculated using (3.17).

$$Distance\ Error = \sqrt{\Delta X^2 + \Delta Y^2} \tag{3.17}$$

In every cycle, the target θ is calculated using (3.18), and the error of θ is found using the difference between actual θ and target θ.

$$Target\ \theta\ = \frac{\Delta Y}{\Delta X} \cdot \frac{180}{\pi} \tag{3.18}$$

After position and angle errors calculation, the controller calculates new linear and rotational speed of the robot. These desired robot speeds are converted to the rotational speed of wheels using the inverse kinematic model.

The rotational speed of wheels is converted to PWM values, using a kind of open-loop speed controller designed to obtain the PWM input values for the desired speed.

This speed controller comes from an experimental procedure that uses a 1D lookup table data after an experimental characterization of the robotic actuation system. The saved 1D lookup table allows delivering the right PWM value for a desired rotational speed. PWM signals are sent to the robot drivers generating the required rotational speed that is, then, measured by encoders. Actual rotational speeds of each motor are used in the kinematic model to find actual positions and orientation of the robot.

In addition to the orientation information given by encoders, redundant measurements are coming from IMU sensors. IMU sensor measurements use a Kalman filter to get more stable measurement values and value with less noise. Encoders, IMU measurement and Kalman filtered are combined to give the actual orientation of the robot. After the position and orientation calculations, position and angle error position are calculated again, as illustrated in Figure 3.5.

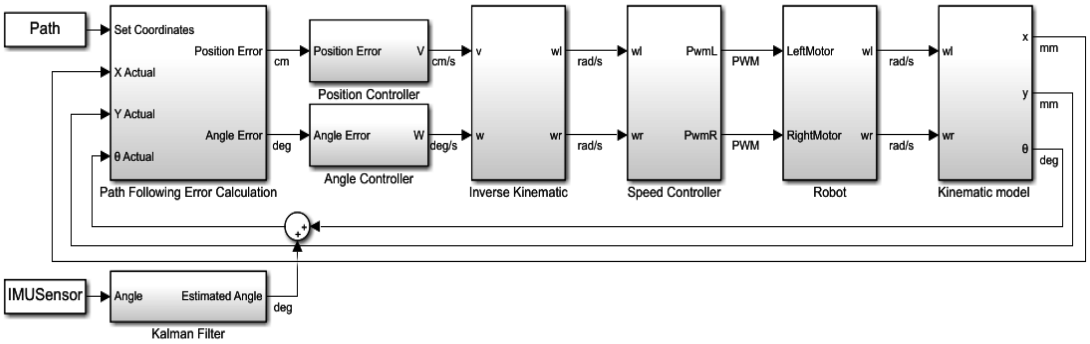

Figure 3.5 Control Algorithm Block Diagram.

3.5 Open-Loop Speed Controller

The results of experimental characterization of the climbing robot actuation system were performed. The actuation system includes motor, pallets and the complete mechanisms of the robotic body. Data of the experimental procedure is saved in a lookup table. This lookup table has information on PWM commands vs. rotational speed. There is given PWM signal to motors then rotational speeds are calculated. This look-up table must be filled with real-time experimental procedure, data obtained while the climbing robot is climbing a vertical wall, and in a working situation. During this operation, climbing robot climbed upward and downward on the metallic sheet. Since the main objective is to provide the necessary PWM values that generate the right robotic-body speed of a system under load. This table would not work if is filled with theoretical values, which are difficult to model and estimate beforehand, because of the multiples (DC motor, actuation mechanism) model and parameters uncertainties, and for a system under high disturbance. Figure 3.6 and Figure 3.7 shows each PWM commands for the rotational speed of the left and right motors, respectively.

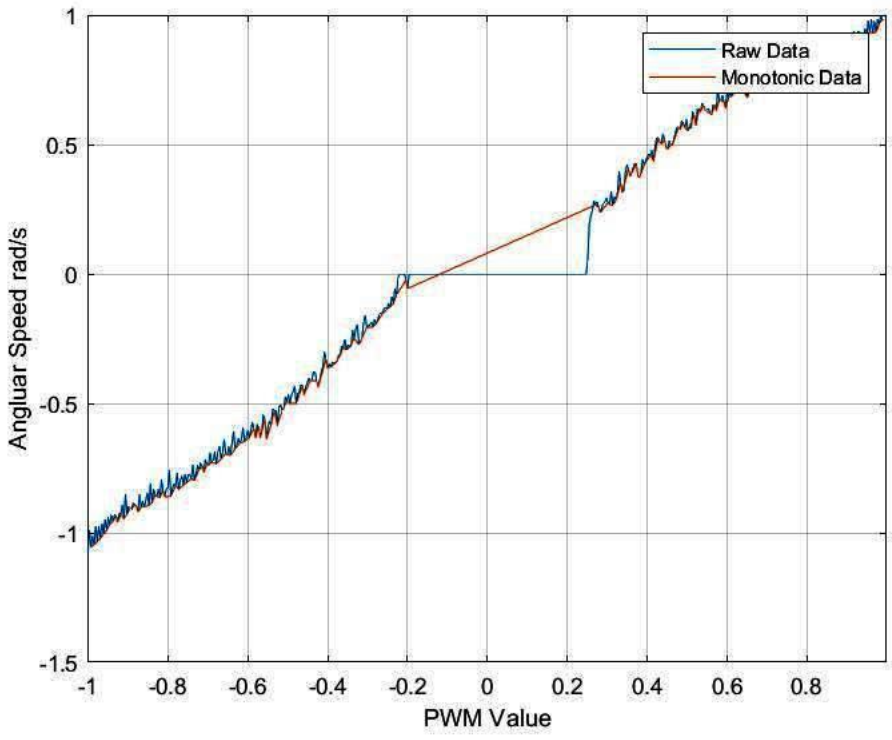

Figure 3.6 Left motor PWM commands with measured angular speed.

Figure 3.6 shows the experimental characterization of the left motor. In our particular experiment, the dead-zone is measured at -0.2 and 0.24 PWM for wise and counter wise movements. The maximum angular speed goes to 1 rad/s.

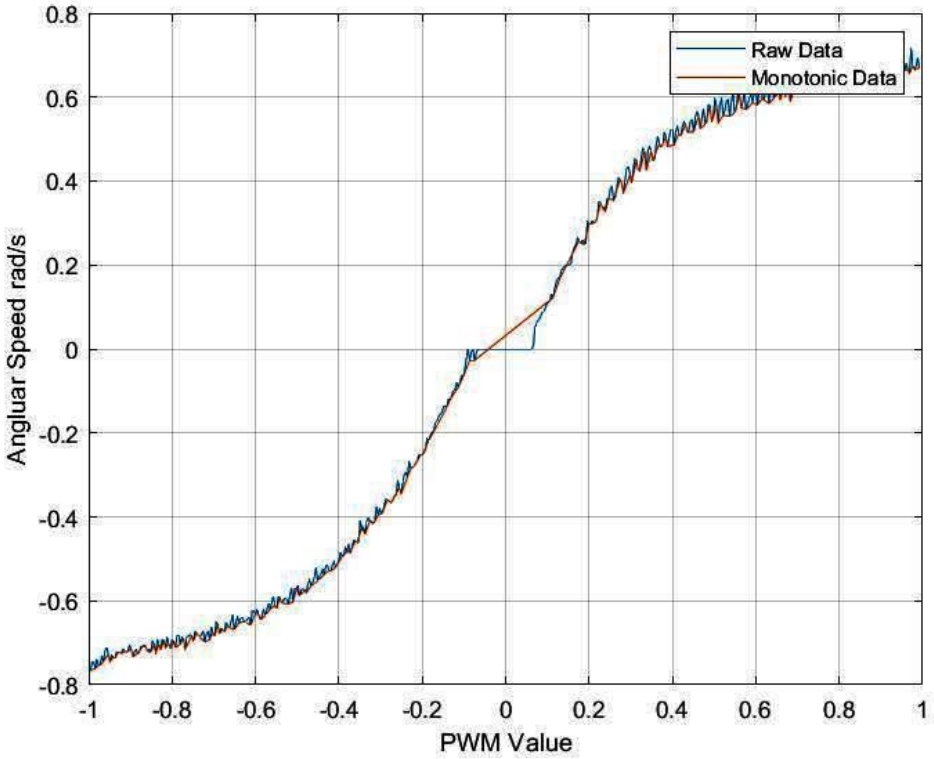

Figure 3.7 Right motor PWM commands with measured angular speed.

Figure 3.7 shows the experimental characterization of the right motor. The right motor dead-zone is -0.1 and 0.06 PWM for wise and counter wise movements. The maximum angular speed is 0.78 rad/s.

3.6 Closed-Loop Controller for Linear Speed and Angular Speed

Two PID controller are used for left and right actuation system, as shown in Figure 3.8(a). The position and angle control blocks make use of PID regulators to correct the obtained error, and generate the necessary control signals for both linear speed (cm/s) and angular speed of the robot (deg. /s), see Figure 3.8(b).

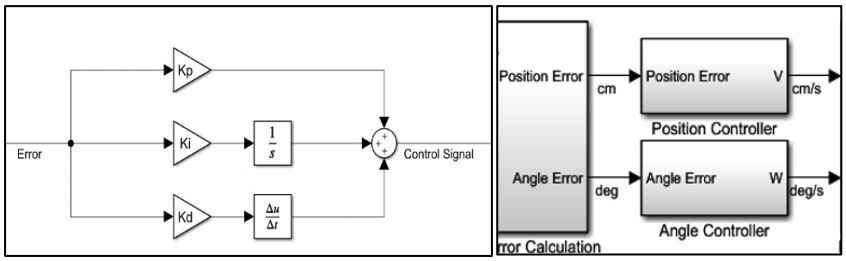

(b) (b)

Figure 3.8 Control regulators: (a) PID scheme and (b) the use of linear speed and angular speed regulators.

3.7 Experimental Validation of the Control Strategy

The following are experiments performed to validate the proposed control method. The set up starts by giving the initial coordinate values X: 0cm, Y: 0cm, θ: 0° as an initial reference and the desired set point was established to move the robot to new values X: 50 cm. Y: 30 cm. The path is way-points then generated for tracking, as shown in Figure 3.9.

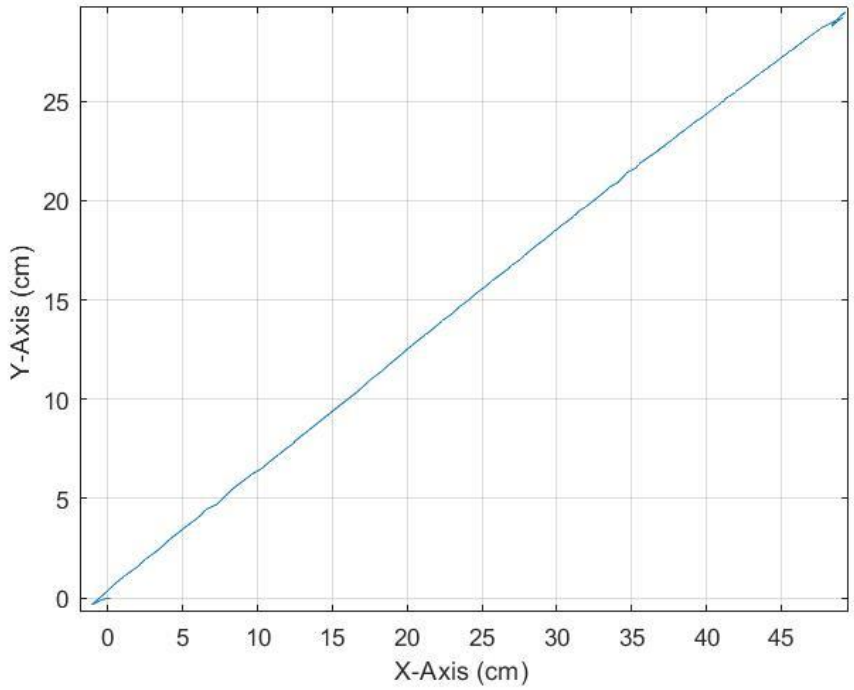

Figure 3.9 Setting the initial point and the desired reference for tracking.

Robot's initial state is established, and then, it starts to move to the target position.

Firstly, the robot places the head angle, and then it goes to the target position. If the angle PID controller's proportional gain is small, the robot moves in a curvilinear path. But, if the proportional gain is greater, the robot moves directly to the target position, as it is shown in Figure 3.9.

The PID gains are chosen experimentally looking for the fast and accurate way to the target position, and considering do not saturate the motor to perform the manoeuvre. The controller gains were selected as follows:

- Position Controller: $K_p = 0.04, K_i = 0.2\ K_d = 0.01$
- Angle Controller: $K_p = 0.05, K_i = 0.01\ K_d = 0.001$

Figure 3.10 and Figure 3.11 show the control performance when controlling the angular position for the left and right motor, respectively. In Figure 3.10, the generated trajectory named as WleftSet, and the measured control response WleftActual is shown. This figure also shows the required control effort, named as Duty Cycle, to perform the manoeuvre. Similarly, Figure 3.11 illustrates the performance of the angular velocity of the right motor.

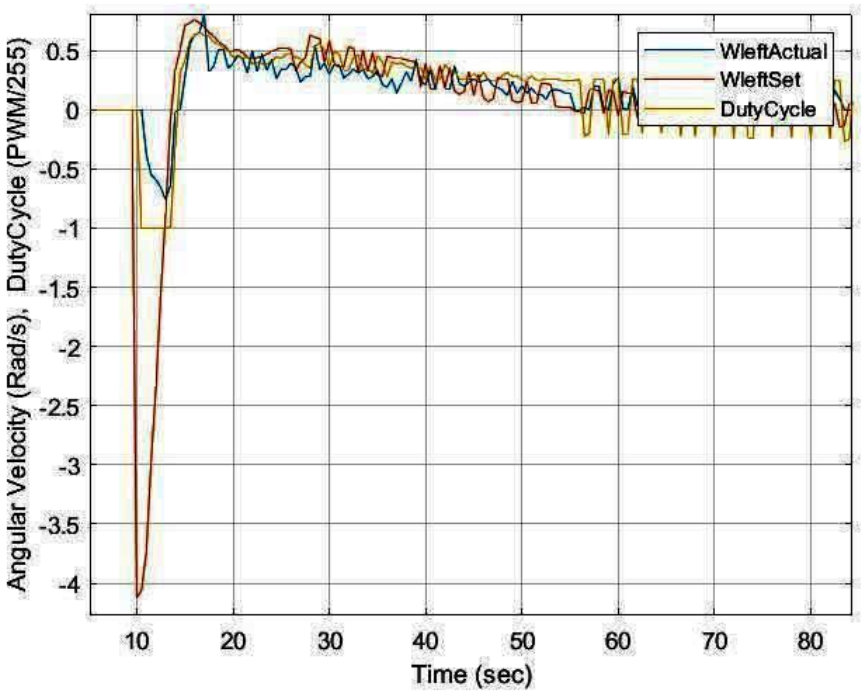

Figure 3.10 Control performance: angular speed of the left motor.

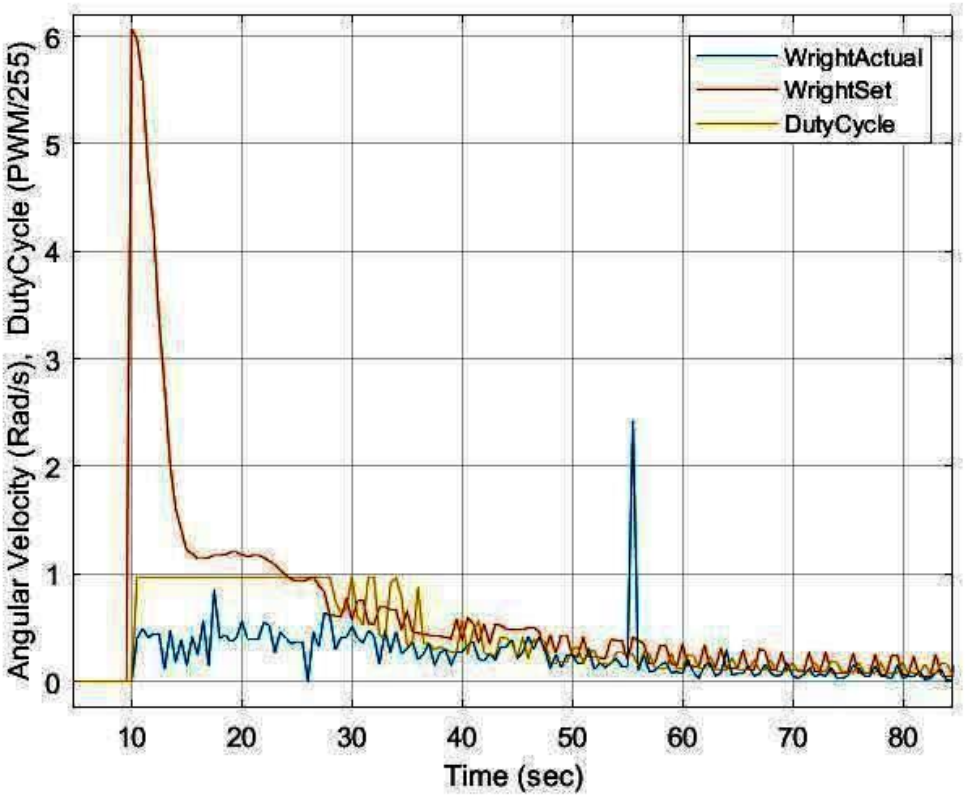

Figure 3.11 Control performance: angular speed of right motor.

In both figures, the performance of the speed controller's response of the system is depicted. Figures show saturation constrain in the transient. This issue will affect the control speed response but is not very serious in the permanent regime response. The control signal is limited. Part of the control signal is used for controlling the angular speed of the robot. But the rest has to be shared with the head angle controller (see Figure 3.12). Figure 3.12 depicts the reference given to the head angle controller (Set angle) and is compared to actual angle measurements.

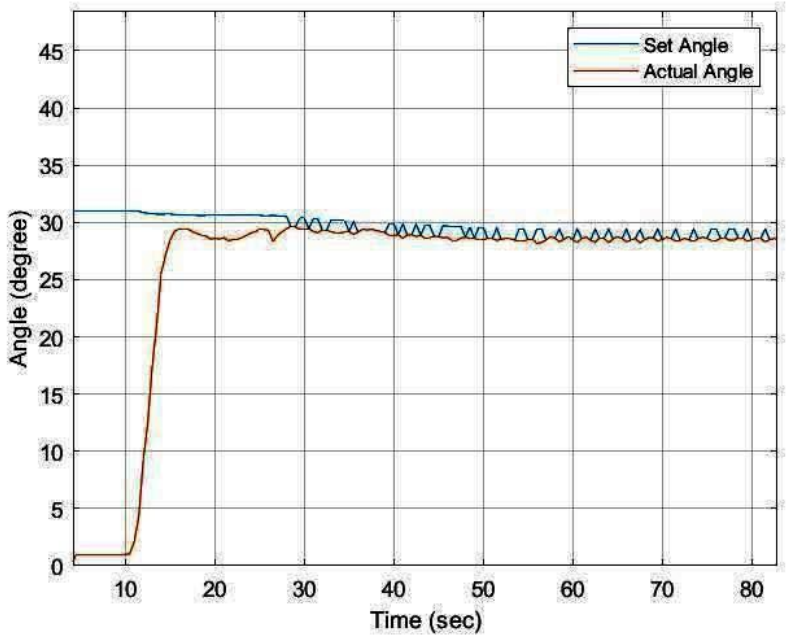

Figure 3.12 Head angle control performance.

Once the settle head angle is reached, the robot goes to track target position, as shown in Figure 3.13. In this figure, the total distance error is depicted in the initial states, and it is decreasing while robot is being closed to the given target position.

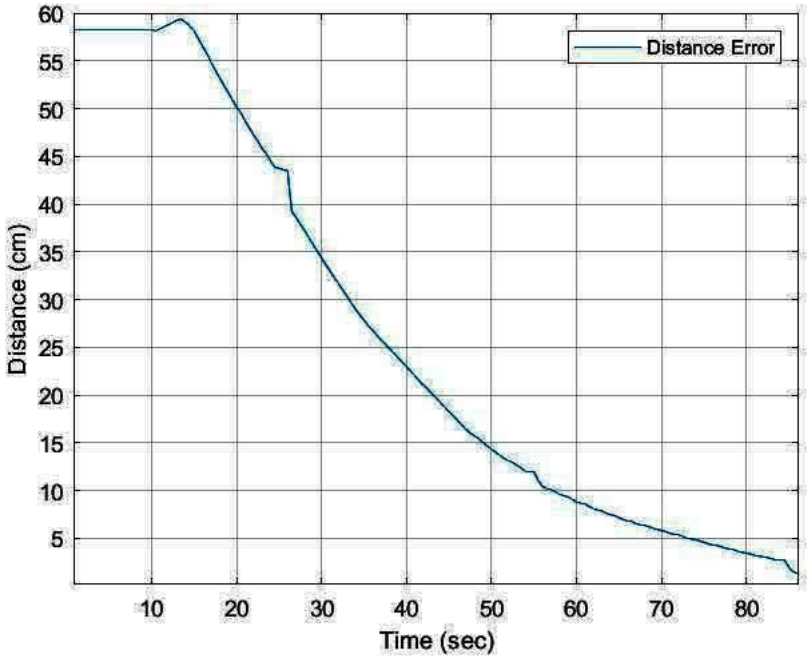

Figure 3.13 Actual distance error changes.

The figures of linear and rotational speeds to manoeuvre to reach the particular target position and robot orientation are shown in Figure 3.14 and Figure 3.15. Figure 3.14 illustrates the linear speed of the robot, while Figure 3.15 shows its angular velocities. Both figures are used to compare the desired (Set Velocity) and measured velocity (Actual Velocity).

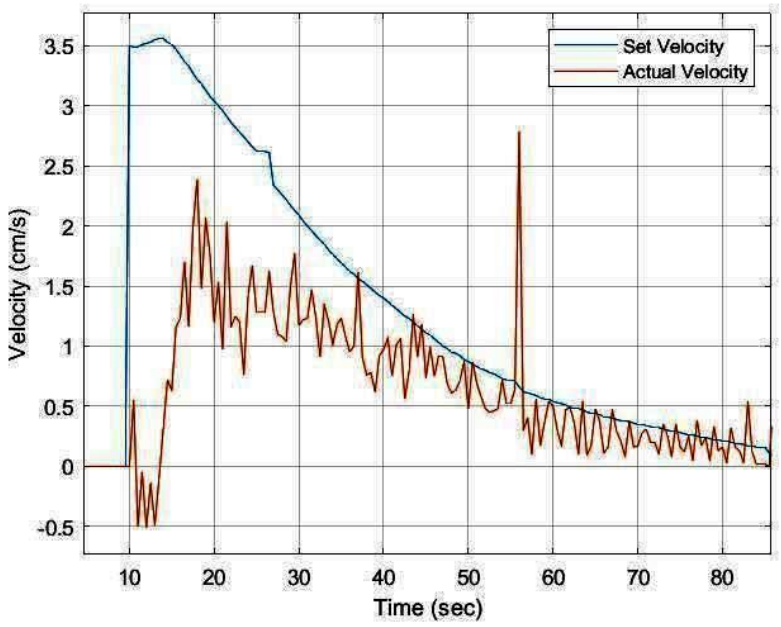

Figure 3.14 Linear speed of robot, comparing desired and actual speed.

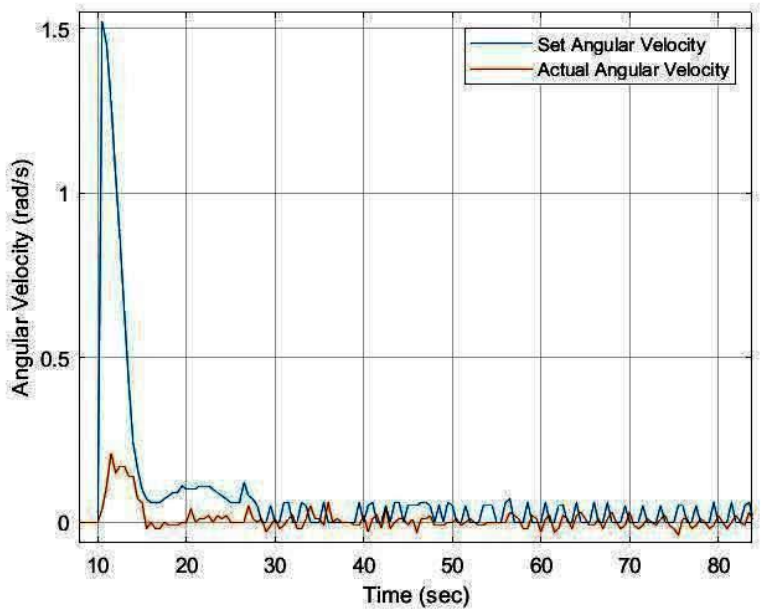

Figure 3.15 Rotational speed of robot, comparing desired and actual speed.

4

CORROSION INSPECTION

In many intensive industrial processes, volatile chemicals like Oil & Gas or petrochemicals are employed. To deposit chemical very high metallic tanks are used, in which the corrosion of the metal sheets is a threat to the longevity of assets. Industrial containers, boilers or pressure vessels wear down due to corrosion that requires monitory systems. The metal corrosion causes leaks or failures and affects the performance and reliability of the facility. Unmonitored facilities may suffer from safety risks, equipment failure, and environmental issues, which cause irreversible loss. There are multiple inspection methods, but in this thesis, a visual inspection of corrosion is studied.

This chapter is outlined as follows: Section 4.1 gives an introduction of the use of cameras for visual corrosion inspection and the use of OpenCV image processing to easily detect corroded areas. Finally, in Section 4.2, multiple test results of corrosion inspection are depicted.

4.1 Corrosion Training and Detection with Image Camera

Our eyes can detect metallic surfaces with corrosion, as shown in Figure 4.1. However, the idea of using a camera and machine learning algorithms is necessary to be part of an automatic robotic inspection. This work illustrates the use of a cascade classifier training with Haar Feature to establish the desired region of diagnosis and to obtain specific feature in each area for classification.

Figure 4.1 Example image of Corrosion.[20]

4.1.1 Cascade Training

Cascade Cascade classifier training is mainly based on Haar Feature. Haar Feature uses rectangular pixels of white and black to understand objects in an image. There is an integral operation for each pixel of an image. Then, the desired pixel size of image is used for examining rectangular features. These rectangular types and an example of object detection with Haar cascades are shown in Figure 4.2. For object detection there is a classification with trained cascade. The rectangles are compared to produce a weight measure. These weights are allowed for comparing each other, and afterward, classified. The classification operation is for every tested image.

In order to test the algorithms, positive and negative corrosion images were used for training. Firstly, all positive images have the same weight, and there are changes for different classification stages. This training goes on until the desired accuracy is reached. In the classification, positive images should be corrosion positive for an efficient performance. In contrast, images without corrosion must be negative.

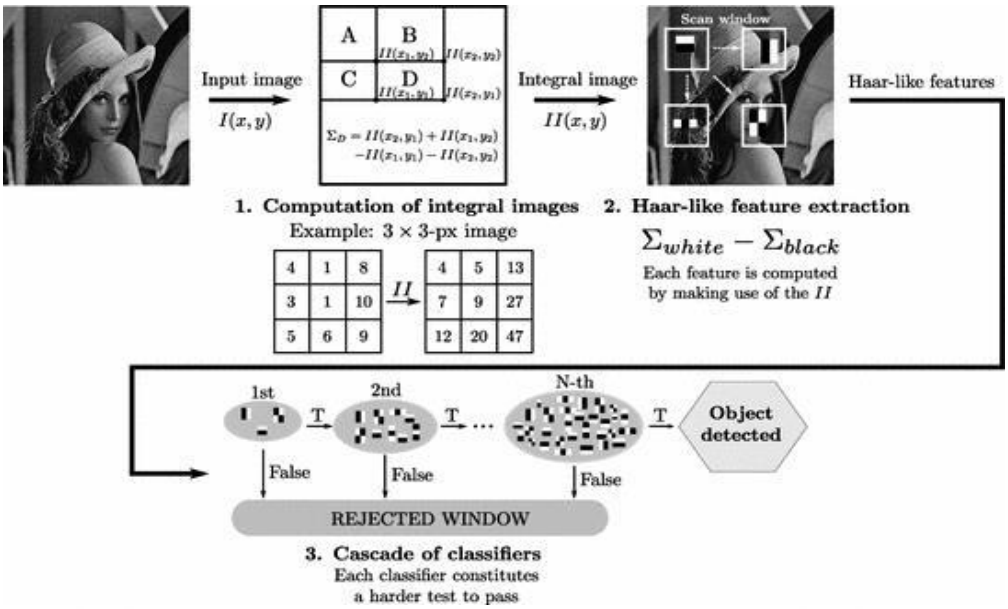

Figure 4.2 Example of object detection with Haar cascades [21].

The following photos are used for corrosion Haar cascade training. The method is used with multiple images with and without corrosion, and the results are depicted in the following figures. The results of positive images are shown in Figure 4.3, while in Figure 4.4, images classify as negative are shown.

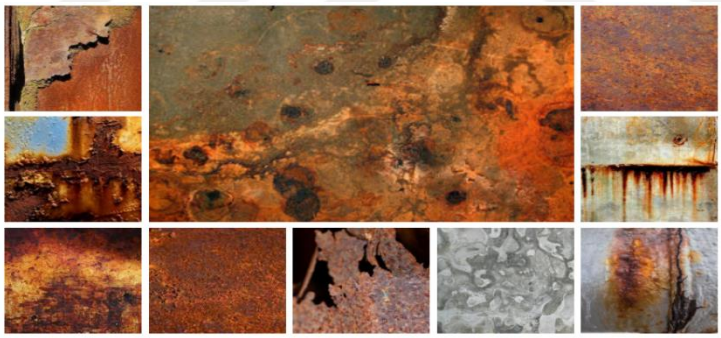

Figure 4.3 Positive images for Training. [22,46]

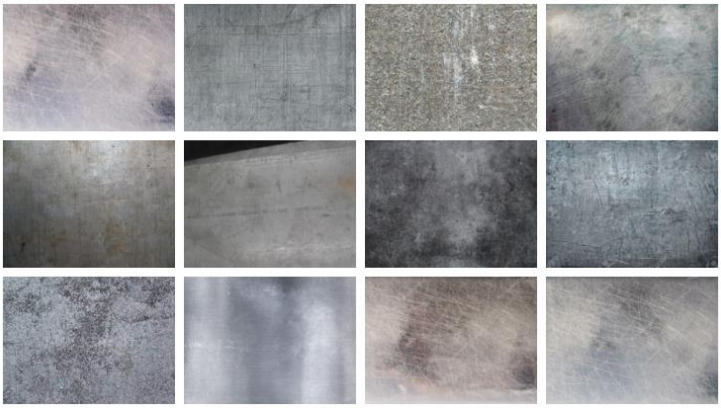

Figure 4.4 Negative images for training. [22,46]

4.1.2 Corrosion Detection

In this work, a trained Haar cascade classifier with opencv image processing libraries were used. Firstly, the desired inspection area is defined and a photo from the camera is shown in Figure 4.5. Afterwards, the image is converted to grayscale as illustrated in Figure 4.6. Employing corrosion Haar cascade classifiers, the obtained positive image with the corrosion is shown using square marks. Finally, when the cascade testing is complete, the image is converted to HSV images. HSV images are used as a tool to illustrate corrosion easily since the detected corrosion areas are depicted in blue rectangles as illustrated in Figure 4.7.

Figure 4.5 Original image for corrosion analysis. [47]

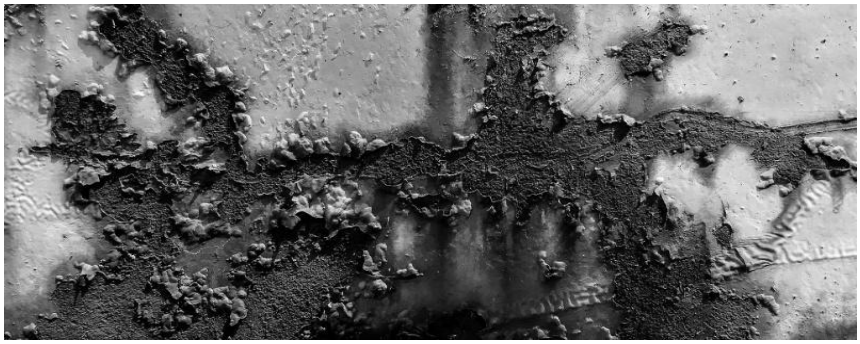

Figure 4.6 Gray scale image is used for cascade detection.

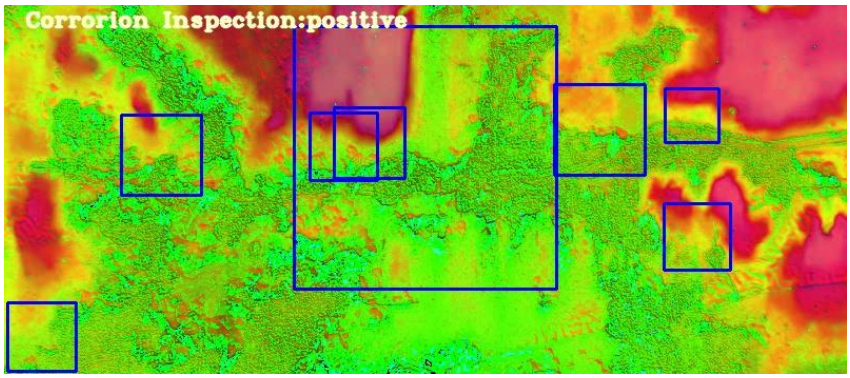

Figure 4.7 HSV coloured image, which is depicted after corrosion analysis for monitory functions.

4.2 Final Test Results of Corrosion Inspection

In the following scenery, a trained corrosion Haar cascade is tested with 20 images of metallic surfaces. Figure 4.8 illustrates the validation of our method to be used with our climbing robot designs. The method shows remarkable test results with an 85% of successful inspection.

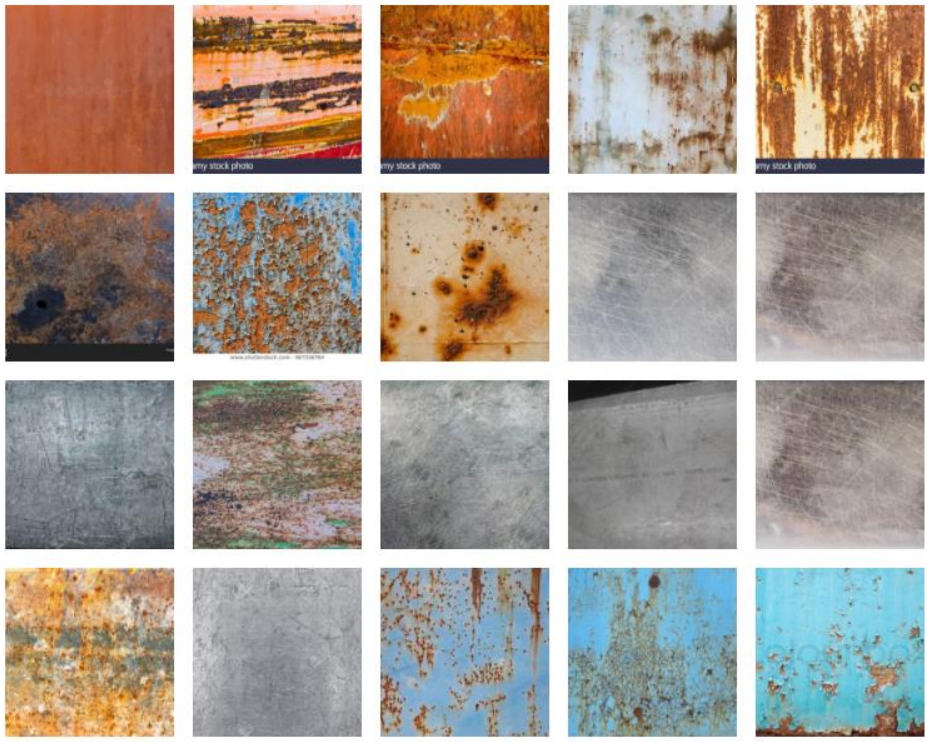

Figure 4.8 Final validation of test images for corrosion inspection. [22-46]

5

A MOTION CONTROL STRATEGY WITH DISTURBANCE OBSERVATION FOR A CLIMBING ROBOT

In this section, a robust motion control strategy for the climbing robot mobility systems that use DC motors is explained. It is a preliminary study to design advanced motion controllers for a climbing strategy. The method is still under development, but some designs from the availed literature were studied, such as the methods in Ohnishi et al. [25], and initial simulations have been performed with successful results.

The simulated environment and general system characteristic are defined here to exemplify our work. The climbing robot has to carry an inspection system to map the surface of oil tanks, and dealing with all constraints of real inspection systems in very challenging working conditions. The robotic body is designed to support all the required equipment to attach the robot to the tank's wall and compensate the effects of magnetic, friction and gravity forces. In this section, some SolidWorks drawings describe the wheel mechanism feature. It is a novel work designed for this particular robotic prototype. This work aims at proposing a control method to be used together with an autonomous positioning strategy. The control system must be robust to all the possible disturbances and noise. The motion control of the robot's wheels must be robust to high perturbation values is therefore proposed. To meet stability and robustness requirements, the method is based on a PD controller and an observer, in which disturbances, such as Coulomb friction and sudden inertia changes are estimated and then compensated. Some simulations of the complete control method for the tracking performance were performed using Matlab/Simulink. The motor transfer function parameters were obtained experimentally and are used for the simulations setup. Remarkable results were achieved by simulating the proposed control method.

5.1 Introduction

The mechanical architecture of the proposed wall-climbing robot is, therefore explained. It includes the frame body, the servo-motors and transmission system, the tracked locomotion system, and hast to consider the permanent magnetic adhesion system. Since adhesive force and Coulomb friction are all changing in nonlinear patterns, the interaction process must have a strong nonlinearity [48][49]. Nonlinear phenomena of the Coulomb friction and the effects of gravity have a strong influence on climbing robots, making it very difficult to control the robot wheels [50].

Innovative methods for disturbance compensation based on observers are well described in the works by Ohnishi et al. [51], and the work by Sira-Ramirez. [53]. The design of DC servo-motor regulators has been one of the bases of multiple mechatronics applications in the industry [51]. A well-designed motion controller of the climbing robot requires proper selection of several devices for sensing and actuation, along with efficient control algorithms. Robust, precise and fast motion is the main target for a climbing robot movement. To compensate the plant nonlinear phenomena, estimation and compensation of the overall disturbances become essential for the control performance [50][52]. A nonlinear position tracking controller with a disturbance observer is proposed to track the desired position in the presence of the disturbance for electrohydraulic actuators. The design of robust servo-motor control with switched observers [53], illustrates enhanced performance because it compensates for un-modelled classical perturbation inputs that affect the observed plant since it exhibits dynamic output reconstruction error injections.

In this chapter, the control strategy made use of a motion controller with disturbance estimation and compensation for uncertain parameters due to the changes in the overall system forces [53]. Furthermore, the control method is designed to cope with load disturbances. The proposed control was studied by carrying out simulations using Matlab/Simulink. This approach guides us in the prospect of using robust motion control algorithms for climbing robots.

5.2 Climbing Robot Design Characteristics

A descriptive design of the robot mechanisms is presented here. The robotic body is designed to support the magnetic adhesion system to attach the robot to the metallic sheet. A novel mechanical system uses wheels that rotate changing the instantaneous centre of rotation.

The robot climbs up and dawns the wall, it goes right and left by configuration its wheels and maintaining the centre of gravity (Climbing Robot + inspection system). It keeps the robot into a safe state that increases the stability and security of the system. Some of the system components are designed as follows:

- Motors: there are 4 DC motors (with reduction and encoder) and 2 Servo motors to drive the wheels 180-degree right-left movements, as shown in Figure 5.1(a).
- Electromagnets: used for generating a normal force to attach the robot to the climbing surface, keeping the full robot apparat closed to the wall; see Figure 5.1(b).
- Wheels: the rotation mechanism is a critical problem in mobile robots, because of the high magnetic forces, the gravity forces, the non-linearity because of Coulomb friction forces and saturation boundaries, in addition to model parameter uncertainties. Figure 5.1(b) illustrates the characteristics of the wheels. The design in this proposes and simulates a possible wheel configuration solution.

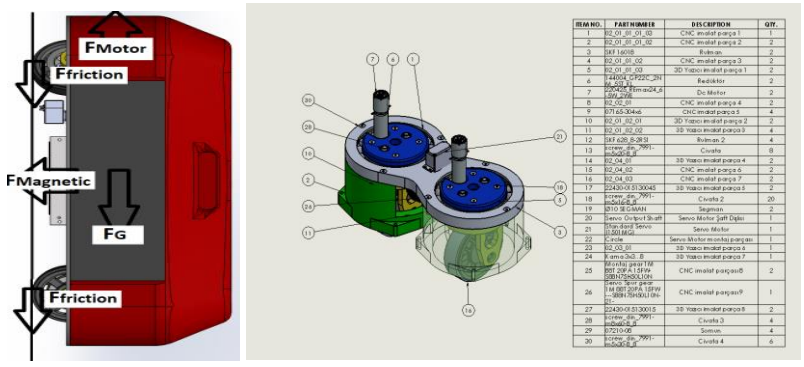

(a) (b)

Figure 5.1 Solidwork drawings of the climbing robot: (a) the system forces acting on the robot, and (b) wheels mechanism

Sensory system: the robot is enhanced with a sensor fusion, which is used to obtain information about the operating state of the control system, its working environment and used for trajectory planning. Some of the required sensors are ultrasonic distance sensors, capacitive sensors, IMU sensors, and a camera is needed for corrosion inspection.

5.3 Control Method

The control method consists of the following:

- The use of a PD controller and an algorithm that generates 8th order polynomial references (Bezier curves to be used as a reference).
- Disturbance observer estimation and the use of a compensation term.
- The robot position is estimated through a Kalman filter that uses measurements from different sensors for calculating the angle of the robot's head, and these position values give feedback to the control system [54].

The system disturbance is caused by multiple reasons, load variations, motor parameter uncertainties, additional load torques, Coulomb friction, gravity force, and strong magnetic forces. On the other hand, the system provides a feed-forward term included to accelerate the dynamic response. Figure 5.2 is a block diagram of the necessary step of the complete control design.

5.3.1 DC Motor Dynamics

$$J\ddot{\theta} = K_t V - \Gamma_f(\dot{\theta}) \tag{5.1}$$

K_t is the motor torque coefficient of the electric motor, V is the voltage signal, J is the inertia load, θ is the motor angle, $\ddot{\theta}$ is the motor acceleration and $\Gamma_f(\dot{\theta})$ is the friction torque in function of the angular speed [55]. V stands for the voltage signal which is a control variable and the input to the servo-amplifier that regulate the motor current. The motor electrical dynamics are faster than the mechanical dynamics; therefore, we consider only the mechanical model. $\Gamma_f(\dot{\theta})$ is expressed as follows

$$\Gamma_f = \begin{cases} g(\dot{\theta}) & \text{if } \dot{\theta} \neq 0 \\ \Gamma_s \text{sgn}(\dot{\theta}) & \text{if } \dot{\theta} = 0 \text{ and } |V| \leq \dfrac{\Gamma_s}{K_t} \end{cases} \qquad (5.2)$$

$$g(\dot{\theta}) = \text{sgn}(\dot{\theta})\Gamma_c + \text{sgn}(\dot{\theta})(\Gamma_s - \Gamma_c)e^{-\left(\frac{|\dot{\theta}|}{v_s}\right)} + \nu\dot{\theta}$$

Γ_s is the static friction torque (which causes the stiction phenomena at $\dot{\theta} = 0$). Γ_c is the coulomb friction, which takes place during the movement, and is constant independent from the speed. v_s is the Stribeck velocity and it denotes the sliding velocity, where only a 37% of the static friction torque is active. Finally, ν is the viscous friction coefficient.

5.3.2 State-Space Model of the DC Motor and a Reduced Disturbance Observer

In order to give to the system a realistic behaviour of a motor model, some disturbance elements must be taken into account. In this work, the simulated perturbation include inertia changes and the friction torques. These perturbations cause most of the problems in motion control. Non-zero steady error and overshooting are clearly consequences of these disturbances.

$$J = J_o + \Delta J, \qquad K_t = K_{to} + \Delta K_t \qquad (5.3)$$

Where J_o and K_{to} are the nominal inertia and nominal motor torque constant respectively. The ideal transfer function of the DC motor plant is considered to be *G(s)* for a system without perturbation.

$$G(s) = \frac{\theta(s)}{V(s)} = \frac{K_{to}}{J_o s^2} \qquad (5.4)$$

Replacing (5.3) into (5.1) the following can be stated:

$$G(s) = \frac{\theta(s)}{V(s)} = \frac{K_{to}}{J_o s^2}$$
$$\tilde{d} = -\frac{1}{J_o}\left(\Gamma_F + \Delta J\ddot{\theta} - \Delta K_t V\right) \qquad (5.5)$$

Where $\tilde{d}$ stands for the system disturbance. An augmented state equation can be build, a system that considers the state space model of the DC motor plant and the disturbance:

$$\frac{d}{dt}\begin{bmatrix}\theta\\ \dot{\theta}\\ \tilde{d}\end{bmatrix}=\begin{bmatrix}0 & 1 & 0\\ 0 & 0 & 1\\ 0 & 0 & 0\end{bmatrix}\begin{bmatrix}\theta\\ \dot{\theta}\\ \tilde{d}\end{bmatrix}+\begin{bmatrix}0\\ \frac{K_{t0}}{J_0}\\ 0\end{bmatrix}V^{ref} \tag{5.6}$$

Since the motor angle signal can be obtained with an encoder, a reduced-order observer can be used. The state space equation of this observer is well explained in the work by Ohnishi et.al [51], in which the following observer is stated:

$$\frac{\mathrm{d}}{\mathrm{dt}}\begin{bmatrix}z_1\\ z_2\end{bmatrix}=\begin{bmatrix}k_{11} & 1\\ k_{21} & 0\end{bmatrix}\begin{bmatrix}z_1\\ z_2\end{bmatrix}+\begin{bmatrix}-(k_{11}{}^2+k_{21})\theta+{K_{t0}}/{J_0}\,V\\ -k_{21}k_{11}\theta\end{bmatrix} \tag{5.7}$$

With the use of the observer's states variables (z_1, z_2), k_{11} and k_{21} are free parameters, and the system output θ, the disturbance is estimated.

$$\hat{\tilde{d}} = -k_{21}\theta + z_2 \tag{5.8}$$

If we want both observers' poles to be allocated in the same place (- β) on the negative real axis at the complex plane, we must define:

$$k_{11} = -2\beta, \qquad k_{21} = -\beta^2 \tag{5.9}$$

If the observer is fast enough the estimation of $\tilde{d}$ and its compensation can be performed. As seen in Figure 5.3, the input signal to the system is

$$V = V_o - \frac{J_0}{K_{to}}\hat{\tilde{d}} \tag{5.10}$$

Replacing (5.10) in (5.4), and with the assumption that $\hat{\tilde{d}} \cong \tilde{d}$, a simple second order system is obtained which is an ideal DC motor second order function *G(s):*

$$\frac{\theta}{V_o} = \frac{K_{to}}{J_o s^2} \tag{5.11}$$

Making use of (5.11) a Feed-forward term can be easily defined where F(s) is said to be $G(s)^{-1}$

$$F(s) = \frac{J_o s^2}{K_{to}}$$

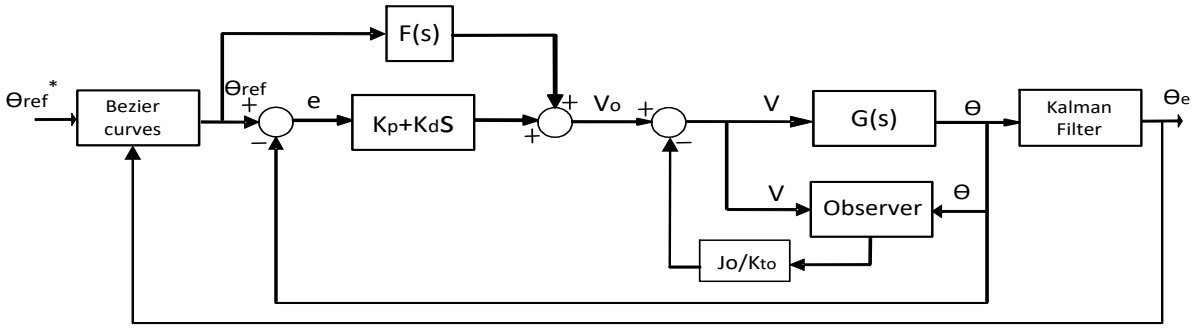

Figure 5.2 Complete control method: Bezier curves, PD controller , feed-forward term, disturbance observer and its compensation, Kalman filter and the DC motor plant + disturbance.

5.4 Control Method Simulation

5.4.1 Simulation Setup

Matlab/Simulink was used to program, compiled and uploaded to the digital acquisition board MKR1000, which is connected to an MKRMotorCarrier and a DC motor set (motor+reduction+encoder). The motor nominal parameters were obtaining by means of experiments. After identifying the static Coulomb torque, the Parameter Estimation Toolbox of Matlab was used to identify the nominal motor parameters. The motor nominal parameters are listed in Table 5.1.

5.4.2 Control Method Results

The simulation uses real DC motor-set and evaluates a motion control method robust to high disturbance values. This includes a PD regulator and an observer to be used for a climbing robot previously explained. The Coulomb friction was programed as explained in (2), and the nominal inertia, as well as a sudden change of the inertia at time=2s was added to evaluate the system performance. The disturbance observer's poles were placed in *P*, and PD controller poles $S_{1,2}$ were calculated for obtaining fast critical damped responses. The poles values have been chosen considering the system boundaries sampling time t_s=0.001s and motor saturation V_{sat} of a real platform. The system makes use of 8th order Bezier

polynomial (0 to pi/6). The control and some general simulation parameters are given in Table 5.1 .

Table 5.1 System Parameters

Motor Parameters	**Value**	**Variation Range**
Motor axis inertia (J_0)	0.01354 Kg. m^2	$0-2300\%$
Motor constant (K_{t0})	0.474 N. m/V	$\pm 10\%$
Coulomb friction torque(Γ_c)	0.072 N. m	$\pm 0.1 N.m$
Static friction torque (Γ_s)	0.1 N. m	$\pm 0.15 N.m$
Viscous friction (v)	0.3792 $\frac{\text{N. m. s}}{\text{rad}}$	$\pm 1\%$
Stribeck velocity (v_s)	0.05 rad/s	N.A.
Control Parameters		
Disturbance Observer's poles	$p = -300$	
PD controller poles	$s_{1,2} = -100$	
Gains	K_p= 285 K_d=5.71	
Sampling time	t_s=0.001s	
Motor saturation	$Vsat = 1$ V	

Figure 5.3 shows the motion control response for the complete method, a PD control with a disturbance compensation term. In this figure, the required control effort is also depicted, the control signal only reaches a maximum when the trajectory starts, a value that can be provided by maximum stall torques, and subsequently, the control signal is under saturation. Figure 5.4 illustrates a remarkable observer performance, a fast and accurate estimation of the disturbances for the whole simulated time, which takes account of trajectory initial, transient and steady states, in addition to the efficient position tracking when the inertia changes suddenly at t=2s.

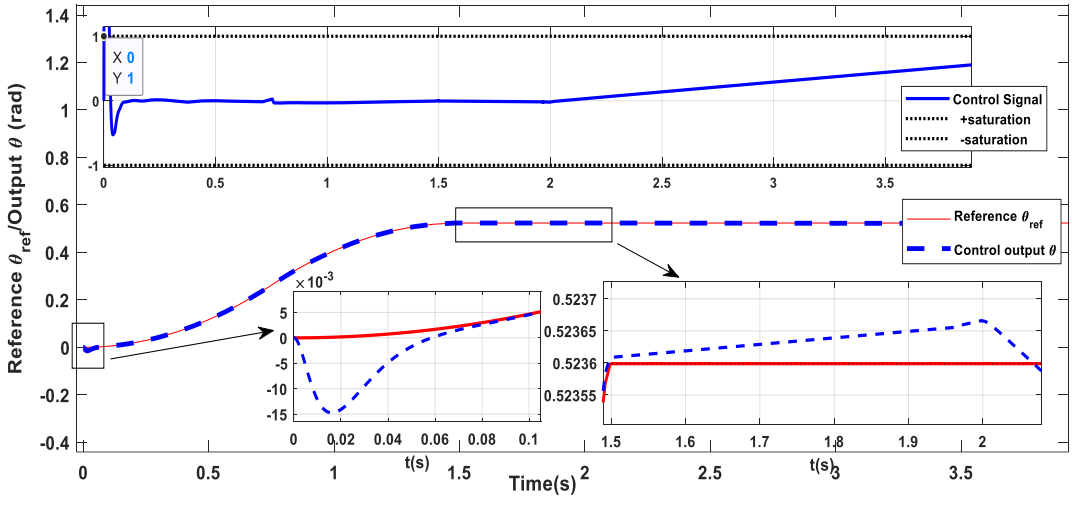

Figure 5.3 Motion Control Response

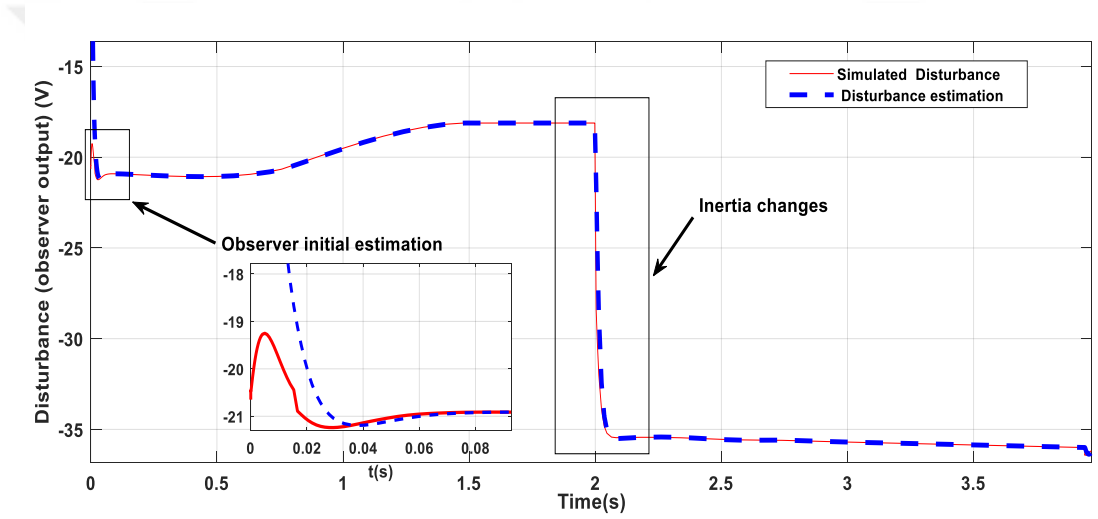

Figure 5.4 Observer performance

The overall disturbance is estimated by the observer and then compensated. Two loops are considered an inner loop with the PD dynamics and an outer loop that gives a fast response and exhibits remarkably tracking performance robust to Coulomb friction and changes of the system inertia.

5.5 Conclusion

A robust motion control method for the wheels of the climbing robot is designed and simulated. This is a preliminary study of motion control for the advanced mechatronic system. The disturbance observation method has been obtained from literature and some simulation of the DC motor system with perturbation have been considered and simulated. This consists of an inner loop, with the PD control

dynamics, an outer loop with a fast response and exhibits remarkably tracking performance robust to high disturbance. In order to satisfy the system performance, the overall disturbance is estimated by an observer and then compensated. The simulated perturbations include inertia changes and the friction torque. In order to make realistic simulations, real system sample-time must be established, and the motor saturation limits must be also experimentally obtained and used in the simulation.

Further work includes a mathematical demonstration of all the method equation, evaluation of the system robustness and the experimental validation of our methods using the real-time climbing robot platform.

6

RESULTS AND DISCUSSION

The list of conclusions and contribution drawn from the thesis are explained in this chapter.

6.1 Conclusions with Regards the Mechanical Design

- A novel mechanical design of a climbing robot was designed and built. It is a palletized robot that uses DC servomotor for the system actuation. The proposed design uses magnetic adhesion to attach the robotic body to the metallic wall. All the necessary robotic mechanisms were designed and Solidworks drawings described the robot's mechanism features.
- In order to evaluate the mechanical behaviour of the system, numerous experiments were performed. The experimental validation established the capabilities of the climbing robot to confront the vertical climbing, and to provide satisfactory mobility.

6.2 Conclusions Appertaining to Software, Hardware and Sensory System of the CRMS

- The thesis describes a robotic prototype with the necessary hardware, software and sensory system for robot positioning and locomotion.
- A sensorial system strategy to estimate the angle of the robot's head was proposed. The robotic design is suitable to be used along with the robot a motion positioning strategy, and especially, the sensory system is robust to all the possible disturbances that may come from magnetic noise. This study is used in our design for an autonomous tracking and a mapping system powered by a sensor-fusion, which consists of inertial measurements, kinematic models and a Kalman filter.
- Multiple experiments were performed to validate the sensory system and to validate the performance of them on the robot while performing climbing. The sensory system and its tracking capabilities were tested using a control

strategy. This mobile robot uses additional sensors to deal with the localization problem; therefore, we have enhanced the robotic system with encoders, IMU sensors to correct some of the localization problems.

6.3 Conclusion Appertaining to the Programming Architecture of the CRMS

- A programing architecture based on Node-Red architecture is used for the communication between appliances and control purposes was programmed. It is Node-Red architecture that incorporates advanced reconfigurable control tools and acquisition systems.
- The designed system has a web-based user-interface and can connect the robot via a mobile phone or a pc. The climbing robot and the user can be connected to the same wireless network, and the system allows for manual operation.

6.4 Conclusions with Regards the Design of a Control System

- A control strategy for driving a differential CRMS was proposed and implemented. This strategy was based on an experimental procedure to characteristics of the actuation system as a whole (motor-reduction, pallets, and related mechanisms), and that uses a 1D lookup to generate data PWM vs speed outputs. This first approach has been denominated as open-loop speed control.
- Encoders, IMU sensor measurements, and a Kalman filter are combined to give the actual orientation of the robot. Experiments show that with the proposed sensor fusion, the filtered head angle is calculated accurately.
- PID Closed-Loop Controllers for linear speed and angular speed of a differential robot was proposed. Numerous experiments were carried out to evaluate the control method. In these experiments, the robot locomotion and the posture were controlled obtaining notable results. To evaluate overall performance some criteria are defined, such as the system response when controlling the angular and linear velocities, the head angle control performance, the total error in the way-point tracking, and the left and right angular speed with control signal requirements. The results validate the system efficiency for the

designed task performed. However, further works must consider a better control system for robust and efficient robot mobility and inspection.

6.5 Conclusions Appertaining to Methods for Corrosion Inspection

- Camera-based system is used for the inspection system that provides pictures of the metallic surface and corrosion samples to be processed and worked along with machine learning algorithms.
- Python with OpenCV libraries are integrated for image processing. The system uses Linux execute commands at Node-Red to work with Python Script of image processing.
- Some methods were carried out for corrosion inspection, such as cascade training and classification. A simple framework is used to produce an efficient classification, and to reduce false positive detection. The training was done using corrosion figures and Haar cascade training. This work uses "corrosionhaarcascade.xml" with OpenCV image processing libraries. The final system can define an inspection area, and the image is converted to grey. When the cascade testing is complete, the image is converted into an HSV image with corroded areas. This method produced successful results giving us the prospect of using these methods to enhance our robotic system with corrosion inspection capabilities.

6.6 Conclusions Appertaining to the Design of Motion Control for the CRMS's Wheels Robust to High Perturbations

- A robust motion control method for the wheels of the climbing robot is proposed and simulated. It is a preliminary study of motion control for the advanced mechatronic system. The disturbance observation method has been obtained from literature, and some simulation of the DC motor system with perturbation have been considered and simulated.
- The control strategy consists of an inner loop, with the PD control dynamics, an outer-loop with a fast response and exhibits remarkably tracking performance robust to high disturbance. To meet the system demands, the overall

disturbance was estimated by an observer and then compensated. The simulated perturbations include inertia changes and the friction torque. To make realistic simulations, a real system sample-time must be established, and the motor saturation limits were experimentally obtained and used in the simulation.

- Further work includes a mathematical demonstration of the method equations, evaluation of the system robustness, and the experimental validation of our methods using the real-time climbing robot platform.

REFERENCES

[1] Yuan Chang and Xiaoqi Chen, "Design of a Scalable Wall Climbing Robot for Inter-plane Traversing", Robotic Welding, Intelligence and Automation, Advances in Intelligent Systems and Computing, vol. 363, 2015.

[2] Schmidt, Daniel & Berns, Karsten, "Climbing Robots for Maintenance and Inspection of Vertical Structures", A Survey of Design Aspects and Technologies. Robotics and Autonomous Systems, vol. 61, pp. 1288–1305, 2013.

[3] Hwang Kim, Dongmok Kim, Hojoon Yang, Kyouhee Lee, Kunchan Seo, Doyoung Chang and Jongwon Kim, "Development of a wall-climbing robot using a tracked wheel mechanism", vol. 22, pp. 1490 1498, 2008.

[4] Wolfgang Fischer, Fabien Tâche, Roland Siegwart, "Magnetic Wall Climbing Robot for Thin Surfaces with Specific Obstacles", Field and Service Robotics, Springer-Verlag Berlin Heidelberg, vol. 42, pp. 551–561, 2008.

[5] David Lattanzi, M.ASCE, and Gregory Miller, "Review of Robotic Infrastructure Inspection Systems", Journal of Infrastructure Systems, vol. 23, September 2017.

[6] Zheng-Yi Xu, Ke Zhang, Xiao-Peng Zhu and Hao Shi, "Design and Optimization of Magnetic Wheel for Wall Climbing Robot", Robotic Welding, Intelligence and Automation, Advances in Intelligent Systems and Computing, vol. 363, 2015.

[7] Tirthankar Bandyopadhyay, Ryan Steindl, Fletcher Talbot, Navinda Kottege, Ross Dungavell, Brett Wood, James Barker, Karsten Hoehn, Alberto Elfes, "A Versatile Multi-Limbed Inspection Robot", International Conference on Intelligent Robots and Systems, 2018.

[8] Shen, Weimin & Gu, Jason & Shen, Yanjun, "Permanent Magnetic System Design for the Wall-Climbing Robot", Applied Bionics and Biomechanics, vol. 4, pp. 2078- 2083, 2006.

[9] K&J Magnetics, Inc, The Original K&J Magnet Calculator page. [Online]. Available: https://www.kjmagnetics.com/calculator.asp?calcType=ring/, 2021

[10] Ensel Elektrik, Cable Weight Calculator page. [Online]. Available: http://www.ensel.com.tr/elkitabi/7 , 2021

[11] The Direnc.net website. [Online]. Available: https://www.direnc.net/ , 2021

[12] VR Tracker, IMU picture page. [Online]. Available: https://vrtracker.xyz/handling-imu-drift/ , 2021

[13] Mobius, Action Camera picture page. [Online]. Available: https://www.mobius-actioncam.com/mobius/wp-content/uploads/2013/08/Mobius-Basic-ActionCam-Pkg.jpg, 2021

[14] The Node-Red website. [Online]. Available: https://nodered.org/ , 2021

[15] The Python website. [Online]. Available: https://www.python.org/ , 2021

[16] Wikipedia, Arduino page. [Online]. Available: https://en.wikipedia.org/wiki/Arduino , 2021

[17] The Amin Ahmadi website. [Online]. Available: https://amin-ahmadi.com , 2021

[18] The Motion website. [Online]. Available: https://motion-project.github.io/ , 2021

[19] Fernández, Raúl & González, Elizabeth & Feliu, Vicente & Gonzalez Rodriguez, Antonio, "A wall climbing robot for tank inspection. An autonomous prototype", Industrial Electronics Conference, 2010.

[20] Flyability, a complete guide to corrosion monitoring page. [Online]. Available: https://www.flyability.com/corrosion-monitoring , 2021

[21] Awad A., Hassaballah M., "Image Feature Detectors and Descriptors." Studies in Computational Intelligence, vol 630, 2006.

[22] Corrosion training and test pictures page 1. [Online]. Available: https://www.bigstockphoto.com/tr/image-367594981/stock-photo-rusted-flat-solid-sheet-metal-surface-background-and-texture-with-leftovers-of-white-paint , 2021

[23] Corrosion training and test pictures page 2. [Online]. Available: https://www.canstockphoto.com/zinc-galvanized-steel-surface-54277182.html , 2021

[24] Corrosion training and test pictures page 3. [Online]. Available: https://www.alamy.com/rusted-flat-solid-sheet-metal-surface-background-and-texture-with-leftovers-of-white-paint-image359215440.html , 2021

[25] Corrosion training and test pictures page 4. [Online]. Available: https://tr.depositphotos.com/221332150/stock-photo-metal-background-texture-titanium-sheet.html , 2021

[26] Corrosion training and test pictures page 5. [Online]. Available: https://www.bigstockphoto.com/tr/image-220815847/stock-photo-grunge-background-from-sheet-metal-background-texture-of-shining-metal-surface , 2021

[27] Corrosion training and test pictures page 6. [Online]. Available: https://www.123rf.com/photo_147909618_rusted-flat-solid-sheet-metal-surface-background-and-texture-with-leftovers-of-white-paint.html , 2021

[28] Corrosion training and test pictures page 7. [Online]. Available: https://www.123rf.com/photo_147909618_rusted-flat-solid-sheet-metal-surface-background-and-texture-with-leftovers-of-white-paint.html , 2021

[29] Corrosion training and test pictures page 8. [Online]. Available: https://hipwallpaper.com/sheet-metal-wallpapers/ , 2021

[30] Corrosion training and test pictures page. [Online]. Available: https://tr.pinterest.com/pin/825777281666716987/ , 2021

[31] Corrosion training and test pictures page 9. [Online]. Available: https://www.123rf.com/photo_110123379_dirty-sheet-metal-texture-silver-aluminum-or-steel-surface-pattern.html , 2021

[32] Corrosion training and test pictures page 10. [Online]. Available: https://previews.123rf.com/images/dmitr1ch/dmitr1ch1802/dmitr1ch180200125/96874537-dirty-steel-sheet-texture-metallic-background-with-damage.jpg , 2021

[33] Corrosion training and test pictures page 11. [Online]. Available: http://www.stainlesssteel-sheetmetal.com/photo/pl16583860-316_stainless_steel_plate_2mm_thick_stainless_steel_metal_sheet.jpg , 2021

[34] Corrosion training and test pictures page 12. [Online]. Available: https://tr.stockfresh.com/image/5427883/texture-of-galvanized-steel-metal-sheet-coated-with-zinc , 2021

[35] Corrosion training and test pictures page 13. [Online]. Available: https://www.dreamstime.com/flat-matte-brown-painted-steel-surface-light-rust-spots-minor-scratches-image184002213 , 2021

[36] Corrosion training and test pictures page 14. [Online]. Available: https://www.shutterstock.com/image-photo/rust-on-painted-steel-surface-467316764 , 2021

[37] Corrosion training and test pictures page 15. [Online]. Available: https://www.alamy.com/rusty-pink-painted-painted-steel-surface-image350084111.html , 2021

[38] Corrosion training and test pictures page 16. [Online]. Available: https://www.123rf.com/photo_100426967_material-of-painted-steel-surface-is-old-rust-.html , 2021

[39] Corrosion training and test pictures page 17. [Online]. Available: https://www.alamy.com/stock-photo-the-surface-of-an-old-painted-rusty-steel-sheet-two-nail-heads-background-140443715.html , 2021

[40] Corrosion training and test pictures page 18. [Online]. Available: https://www.istockphoto.com/tr/foto%C4%9Fraf/beyaz-renk-taraf%C4%B1ndan-boyal%C4%B1-eski-hasarl%C4%B1-metal-veya-%C3%A7elik-y%C3%BCzeyler-gm1139591038-304639955 , 2021

[41] Corrosion training and test pictures page 19. [Online]. Available: https://www.123rf.com/photo_112254644_rust-corrosion-on-metal-surface.html , 2021

[42] Corrosion training and test pictures page 20. [Online]. Available: https://www.alamy.com/stock-photo/rusty-ship-hull.html , 2021

[43] Corrosion training and test pictures page 21. [Online]. Available: https://www.123rf.com/photo_82274902_an-old-white-painted-sheet-of-metal-damaged-by-corrosion-with-spots-of-blue-paint-background-for-you.html , 2021

[44] Corrosion training and test pictures page 22. [Online]. Available: http://texturelib.com/texture/?path=/Textures/rust/painted/rust_painted_0043 , 2021

[45] Corrosion training and test pictures page 23. [Online]. Available: https://www.colourbox.com/image/rusted-metal-wall-background-texture-image-4678198 , 2021

[46] Corrosion training and test pictures page 24. [Online]. Available: https://in.pinterest.com/pin/706854104003659722/ , 2021

[47] Corrosion training and test pictures page 25. [Online]. Available: https://unituffglobal.com/blog/different-types-of-corrosion-in-metals/ , 2021

[48] Zheng-Yi Xu, Ke Zhang, Xiao-Peng Zhu and Hao Shi, "Design and Optimization of Magnetic Wheel for Wall Climbing Robot", Robotic Welding, Intelligence and Automation, Advances in Intelligent Systems and Computing, vol. 363, 2015.

[49] Hwang Kim, Dongmok Kim, Hojoon Yang, Kyouhee Lee, Kunchan Seo, Doyoung Chang and Jongwon Kim, "Development of a wall-climbing robot using a tracked wheel mechanism", Springer Journal of Mechanical Science and Technology, vol. 22, pp. 1490 1498, 2008.

[50] Q. Guo, Y. Zhang, B. G. Celler and S. W. Su, "Backstepping Control of Electro-Hydraulic System Based on Extended-State-Observer With Plant Dynamics Largely Unknown", IEEE Transactions on Industrial Electronics, vol. 63, no. 11, pp. 6909-692, 2016.

[51] Ohnishi, Kouhei & Shibata, Masaaki & Murakami, Toshiyuki, "Motion control for advanced mechatronics", IEEE/ASME Transactions on Mechatronics, vol. 1, pp. 56 – 67, 1996.

[52] Guan and S. Pan, "Nonlinear Adaptive Robust Control of Single-Rod Electro-Hydraulic Actuator With Unknown Nonlinear Parameters", in IEEE Transactions on Control Systems Technology, vol. 16, no. 3, pp. 434-445, 2008.

[53] Sira-Ramirez, Hebertt & Feliu, Vicente, "Robust Σ-Δ modulation-based sliding mode observers for linear systems subject to time polynomial inputs", Int. J. Systems Science, vol. 42, pp. 621-631, 2011.

[54] Acar, Ozgur & Yaşar, Claudia, "Autonomous Climbing Robot for Tank Inspection", 3rd World Conference on Technology, Innovation and Entrepreneurship, Procedia Computer Science, Procedia Computer Science, vol. 158, pp. 376-381, 2019.

[55] Olsson, H. & Åström, K.J. & Wit, C. & Gäfvert, Magnus & Lischinsky, P., "Friction Models and Friction Compensation", European Journal of Control, vol. 4, pp. 176-195, 1998.

PUBLICATIONS FROM THE THESIS

Conference Papers

1. Acar, Ozgur & Yaşar, Claudia, "Autonomous Climbing Robot for Tank Inspection", 3rd World Conference on Technology, Innovation and Entrepreneurship, Procedia Computer Science, vol. 158, pp. 376-381, 2019.

2. Claudia F. Yaşar, Özgür Acar, Şeref N. Engin, "Tırmanan robot için bozucu giriş gözlemleyicili hareket kontrol stratejisi", TOK'2019 Otomatik Kontrol Ulusal Toplantısı, pp. 284-289 ,2019